IMPACT OF LOAD MODELING ON POWER

SYSTEM VOLTAGE STABILITY

By

KISHOR GAIRE

Bachelor of Science in Electrical Engineering

Tribhuvan University

Kathmandu, Nepal

2011

Submitted to the Faculty of the
Graduate College of the
Oklahoma State University
in partial fulfillment of
the requirements for
the Degree of
MASTER OF SCIENCE
December, 2017

IMPACT OF LOAD MODELING ON POWER

SYSTEM VOLTAGE STABILITY

Thesis Approved:

Dr. Nishantha Ekneligoda

Thesis Adviser

Dr. Rama Ramakumar

Dr. Yuanxiong Guo

ACKNOWLEDGEMENTS

I am grateful my thesis adviser Dr. Nishantha Ekneligoda for providing me this opportunity to pursue graduate study at Oklahoma State University. I sincerely thank and admire him for his continuous guidance and support throughout my stay at OSU. Through his consistent suggestions and research directions, I got opportunities to continuously learn and improve myself. I would like to thank the School of Electrical and Computer Engineering for providing facilities and assistantships for my work. I am thankful to my committee members Dr. Ramakumar and Dr. Guo for their constructive suggestions and comments for the improvement of the thesis.

I acknowledge with the highest gratitude to my mom for her encouragements and my dad for his love and kindness. I am thankful to my friends and relatives who helped in different ways in the completion of my thesis. I am heartily thankful to my life partner Rekha for her unconditional love, support, and patience.

Name: KISHOR GAIRE

Date of Degree: DECEMBER, 2017

Title of Study: IMPACT OF LOAD MODELING ON POWER SYSTEM VOLTAGE
                STABILITY

Major Field: ELECTRICAL ENGINEERING

Abstract: Under normal operating conditions, the power system is operated such that acceptable steady voltages are maintained throughout the system buses. However, during disturbances, system voltage deviates from the rated values. A stable system restores its voltage to a stable equilibrium value. However, in an unstable system, the voltage cannot be restored to acceptable steady value, and the system voltage falls progressively. This will force the system into a cascading outage, leading to voltage collapse. It was reported that several blackouts throughout the world were caused due to voltage collapse, which caused huge financial losses and badly impacted social life. As the load models make a significant impact on the voltage stability phenomenon, power system loads are to be modeled such that they closely represent the real system loads. Dynamic load models were used as better load models than static load models for voltage stability study. However, a single dynamic load model cannot represent the dynamics of different types of loads connected to the system. So, aggregated load models such as complex loads were developed which incorporates the models of major types of loads connected in the system. In this thesis, impacts of load models in the static and dynamic voltage stability are analyzed. For static analysis, maximum loadability of power system using different load models are determined using Newton-Raphson power flow method and continuous power flow method. For dynamic analysis, short-term voltage stability is analyzed implementing a various combination of load models. It was observed that short-term voltage stability of the power system largely depends on the types of load and load combinations connected to the system. In static loads, constant power loads have a greater impact on voltage instability than constant impedance type of loads. Dynamic loads such as motor loads support the voltage instability mechanism. It was observed that the voltage collapse occurs for certain combination of static and dynamic loads. However, the voltage collapse was prevented when the combination of loads connected to the bus was changed. Thus, this can be one of the solutions to reduce voltage instability of the power system.

TABLE OF CONTENTS

LIST OF TABLES

LIST OF FIGURES

LIST OF SYMBOLS

$T'_{do}(s)$	d-axis transient rotor time constant
$T''_{do}(s)$	d-axis sub-transient rotor time constant
$T'_{qo}(s)$	q-axis transient rotor time constant
$T''_{qo}(s)$	q-axis sub-transient rotor time constant
H	synchronous machine inertia constant
D	damping constant of the generator
X_d	d-axis synchronous reactance
X_q	q-axis synchronous reactance
X'_d	d-axis transient reactance
X'_q	q-axis open-circuit sub-transient time constant
X''_d	d-axis sub-transient reactance
X''_q	q-axis sub-transient reactance
Xl	armature leakage reactance
$S(1.0)$	saturation factor at 1 pu flux
$S(1.2)$	saturation factor at 1.2 pu flux
T_R	transducer time constant
K_A	voltage regulator gain
T_A	voltage regulator time constant

V_{RMAX}	regulator output maximum limit
V_{RMIN}	regulator output minimum limit
K_E	exciter constant related to self-excited field
T_E	exciter time constant
K_F	rate feedback gain
T_F	rate feedback time constant
$E1$	field voltage
$SE(E1)$	saturation factor at E1
$E2$	field voltage
$SE(E2)$	saturation factor at E2
V_{RMAX}	regulator output maximum limit
V_{RMIN}	regulator output minimum limit
K	governor gain
T_1	controller lag
T_2	controller lead compensation
T_3	governor lag
U_0	opening gate rate limit
U_C	closing gate rate limit
P_{MAX}	upper power limit
P_{MIN}	lower power limit

T_4	delay caused by steam inlet volumes related to inlet piping and steam chest
K_1	1/ per unit regulation
T_5	reheater delay with cold and hot leads
K_2	fraction
T_6	delay due to Intermediate Pressure-Low Pressure turbine, Low-Pressure end hoods and crossover pipes,
K_3	fraction
T_A	fully closing time of intercept valve, v, after fast valving initiation
T_B	time to start to re-open intercept valve, after fast valving initiation
T_C	time to fully re-open intercept valve, after fast valving initiation
P_{RMAX}	maximum mechanical power

CHAPTER I

INTRODUCTION

Transmission lines are subjected to operate at maximum loading to meet the increasing power demand and to obtain a maximum financial return on the investment of transmission lines. If the power system is operated near to maximum power capability of transmission lines without suitable margin, disturbances like faults or equipment outage can trigger voltage instability phenomenon, leading to voltage collapse. Voltage collapse causes detrimental effects in social dimensions and results into a huge financial loss. These are the reasons for major concerns in voltage stability of power system. The authorities responsible for the operation of power system, rely on various parameters to ensure that the system is in stable operation with a suitable margin for voltage stability. The accuracy of these parameters depends on the accuracy of mathematical models representing the dynamics of the power system. This includes the modeling of generators, transmission lines, loads and other devices connected to the power system. Detail modeling of generators and transmission lines are found in the literature for power system analysis. However, it is impractical to implement detail model of each and every load devices connected to the system. Thus, power system loads are modeled as aggregated loads. These load dynamics makes a significant impact on voltage stability [1]. Different load models are proposed to represent more accurate load dynamics. In this thesis, the impacts of various load models are analyzed for static and dynamic voltage stability assessment of power system.

1.1   Background

Voltage instability occurs as the load tends to consume power beyond the amount that can be supplied by the combined generation and transmission system. As the power system cannot supply demanded reactive power to the load, the bus voltage starts to decrease which is the main cause of voltage instability. Unless any immediate corrective actions are taken to restore the system voltage, voltage instability forces the system into a cascading outage leading to voltage collapse. This voltage collapse causes blackouts in the system, which leads to huge financial loss and badly impacts social life. It was reported that several blackouts throughout the world were caused due to voltage collapse. North American blackout on August 14, 2003, and Southern Sweden and Eastern Denmark blackout on September 23, 2003, are the recent major blackouts due to voltage collapse [2]. Due to these blackouts around 50 million people in North America, 1.6 million people in Sweden and 2.4 million people in Denmark were deprived of electricity for several hours before the restoration of the system. This is the reason for major concern in voltage stability of power system.

Voltage stability analysis is done using static and dynamic methods. Common techniques to analyze power system voltage stability are through PV curves and QV curves. Eigenvalues of the reduced Jacobian matrix can be used to analyze power system voltage stability due to small disturbances. The static indices of voltage stability were obtained using the minimum singular value of the Jacobian matrix, model analysis and loading margin [3]. Since voltage instability can occur following the contingency in the system. Voltage stability analysis can be performed through contingency analysis. Also, a loadability limit determination is another technique to analyze the status of voltage stability [4]. This can be done by using the bifurcation techniques, PV and QV curve methods using continuous power flow and using optimization techniques. Moreover, detail phenomenon and analysis methods on voltage instability are given in [4].

The static analysis for voltage stability is mainly based on load flow solutions. In conventional load flow solution using Newton-Raphson (N-R) method, it is assumed that generator connected to slack bus changes its output power to adjust the change in power demand in the system and incorporates all the losses in the system. However, in the actual system, many generators can be involved to supply the system losses and load adjustments. Modification of Newton Raphson method has been purposed with the inclusion of system losses and the slack bus into the Jacobian matrix [5]. Eliminating the slack bus, system losses are distributed to each generator buses but the voltage of all the other buses are measured in reference to a particular bus. This approach would be useful for the power systems with distributed generations. Also, the N-R method cannot converge near to the loadability limit as the Jacobian matrix becomes singular. The singularity problem of the N-R method of load flow was solved by using predictor and corrector process of continuous power flow (CPF) method [6]. Additionally, a new method was proposed to include fourth-order Runge-Kutta method in solving the power flow equations which is superior to other methods in terms of computational time and number of iterations [7].

Besides static analysis methods, voltage stability in the power system can be studied through time domain dynamic simulation and using bifurcation approach [8]. Continuous method and direct method can be used to detect bifurcation points [9]. Different bifurcation points are determined which depends on the type of loads connected to the system. Also, these bifurcation points depend on the adjustment in the reference of voltage controller of the source [10]. Also, [11] utilizes the Fourier analysis and Lyapunov exponents on differential algebraic equations to verify the chaotic behavior of a power system. The FACTS devices can be implemented to control the bifurcations and chaos in the power system through the proper selection of error signal and gain of the controller [12].

Agreement of the results obtained from simulation with that in the real system depends on the accuracy in modeling power system components, mathematical formulation for the analysis and

3

the accuracy of numerical methods to solve the equations. Load modeling is one major concern in voltage stability analysis. Electrical loads are broadly classified into static loads and dynamic loads. Different static and dynamic load modeling were studied [13]-[16] and these load models were used for voltage stability analysis. In [13], the literature on load modeling was generalized and it emphasizes the necessity of dynamic load modeling. The aggregated dynamic load model [15] was presented as the better load representation than the constant impedance or constant power loads. Nonlinear dynamic load model was purposed in [16] and based on these models, voltage sensitivity with reactive power was determined for voltage stability analysis. The system's voltage stability was analyzed by implementing Generic dynamic load model [17]. The list of all the static and dynamic load models proposed to be several researchers, summarized in [14] and [18] can be useful for the comparative study of load models.

Accurate load models require good load modeling approach. The proposed load models involve load equations whose parameters are to be identified for the simulation. This can be done by using component-based or measurement-based approach. In the component-based method, parameters are identified using the physical principle of loads. However, in the measurement-based method, the parameters are chosen such that it closely fits the measured data. Authors in [19] make the comparison of components based modeling approach with the measurement-based approach and stressed on the superiority of measurement-based approach. It also describes the different load models to represent the Induction Machine. The superiority of measurement based method is attributed to the complexity in modeling all the individual loads connected to a power system. In [20], Genetic Algorithm (GA) was implemented for parameter identification of load equations using measurement-based approach and it was observed the superiority of GA method over least square method. The requirements and approaches for better load modeling were explained in [21]. Furthermore, [22] defines disturbance-based load modeling approach. The various aspects to increase the accuracy of load models using measurement-based approach were presented in [23].

Voltage stability phenomenon is affected by load dynamics, Load Tap Changer, Over-Excitation Limiter, etc. Reactive power can be injected into the load bus to prevent the possibility of voltage collapse after a large disturbance. The equation for maximum time delay for this injection was formulated [24]. Active dynamic buffer makes the use of storage battery and capacitors to absorb the transients in the load side [25]. It keeps the constant impedance or constant current on the system side while it supplies constant power to the load. Thus, it decouples the load from the system. This helps to improve the voltage stability of the system.

1.2 Objectives

- ➢ To determine power system loadability limit and to analyze static voltage stability using PV curves and QV curves.
- ➢ To analyze short-term voltage stability for different load models in power system.

1.3 Thesis Outline

The outline of the thesis is as below:

Chapter II: Voltage Stability in Power Systems

This chapter defines voltage stability, voltage instability, and voltage collapse. It presents the concept explanation of voltage instability problem. Static and dynamic analysis methods and the factors affecting voltage stability are discussed. It also presents the voltage instability mechanism of a power system.

Chapter III: Modeling of Power System Devices

This chapter presents the modeling of components connected to the power system used for this research work. This includes the modeling of synchronous generator, exciters, governors and loads.

Chapter IV: Static Voltage Stability Analysis

This chapter presents the static analysis of power systems through PV and QV curves and presents the maximum loadability for different load models in power system.

Chapter V: Dynamic Voltage Stability Analysis

This chapter presents the short term voltage stability analysis through fault-induced delayed voltage recovery for static and dynamic loads.

Chapter VI: Conclusions

This chapter concludes the research work and presents the future scope of research work.

CHAPTER II

VOLTAGE STABILITY IN POWER SYSTEMS

Voltages at all buses of a power system remain within acceptable limit at normal operating conditions. During disturbances, the system voltage fluctuates beyond the acceptable limit for normal operating conditions. If the system fails to restore the voltage after the disturbances, such situation is called voltage instability. As the system is subjected to voltage instability immediate corrective actions must be taken to restore the system voltage into a stable operating point. Otherwise, it forces the system into a cascading outage leading to voltage collapse.

2.1 Voltage Stability Definition and Classification

"Voltage stability is the ability of power system to maintain steady voltages at all buses in the system at normal operating conditions and after being subjected to disturbances" [26]. Voltage stability mechanisms are described using static and dynamic phenomenon.

The static voltage stability is ensured if the steady state operating voltage of the system buses are more than the corresponding bus voltage at the point of maximum loadability. At maximum loadability, the injection of the reactive power into the system increases the system voltage.

In dynamic phenomenon, voltage stability is further classified as small disturbance and large disturbance voltage stability[27]. In small disturbance voltage stable system, voltage

restores near to the pre-disturbance stable state after the system is subjected to small disturbances. The small disturbances are caused due to the small load change in the system, small variations of power generation in the system, etc. In the large disturbance voltage stable system, the system voltage reaches to a post-disturbance equilibrium state, after large disturbances. Large disturbances are caused due to various types of faults in the system, single or multiple contingencies or due to a large change in generations or loads.

Furthermore, voltage stability can be observed as short-term voltage stability and long-term voltage stability. Short-term voltage instability is caused by fast-acting devices such as HVDC and dynamic loads such as motor loads [28]. To analyze short-term stability phenomenon, it is essential to formulate dynamic modeling of loads. This type of instability occurs in the range of a few seconds. Long-term voltage instabilities are caused due to slow acting devices such as tap changing transformers, generator field current limiters and thermostatically controlled loads. This type of instability occurs in the range of a few minutes to several minutes.

2.2   Voltage Stability Analysis in Power System

Voltage stability is a dynamic phenomenon which includes the dynamics of devices connected to a power system. Voltage stability analysis is required for long term and short term planning of transmission lines and operation and control of power systems. The transmission planning engineers should know the maximum capability of a power system with or without contingencies. The power system operator should be aware of the operating condition of a power system at any time which includes the voltage level of all the buses and proximity to voltage instability. Furthermore, the details of a voltage instability mechanism including its cause and effects are to be known to prevent the voltage instability. This information is obtained through voltage stability analysis. Voltage stability analysis can be split into static analysis and dynamic analysis.

| Static Analysis Methods | | Dynamic Analysis Methods |

Linearized DAE model

$$[\Delta\dot{x}] = [A][\Delta x]$$

Modified Load Flow Models

DAE Dynamic Model

$$\dot{x} = f(x, y)$$

$$0 = g(x, y)$$

- Model analysis of state matrix [A]
- Bifurcation Analysis

- Multiple power flow
- Continuous power flow
- Sensitivity analysis
- Identification of voltage collapse point
- Smallest singular value of Jacobian matrix
- Model analysis of reduced Jacobian [J_R]

Solution techniques

- Trapezoid method
- Modified Euler's method
- Variable step method

Global methods

- Bifurcation analysis
- Chaos theory

Small perturbation stability

Large perturbation stability

- Transient Stability
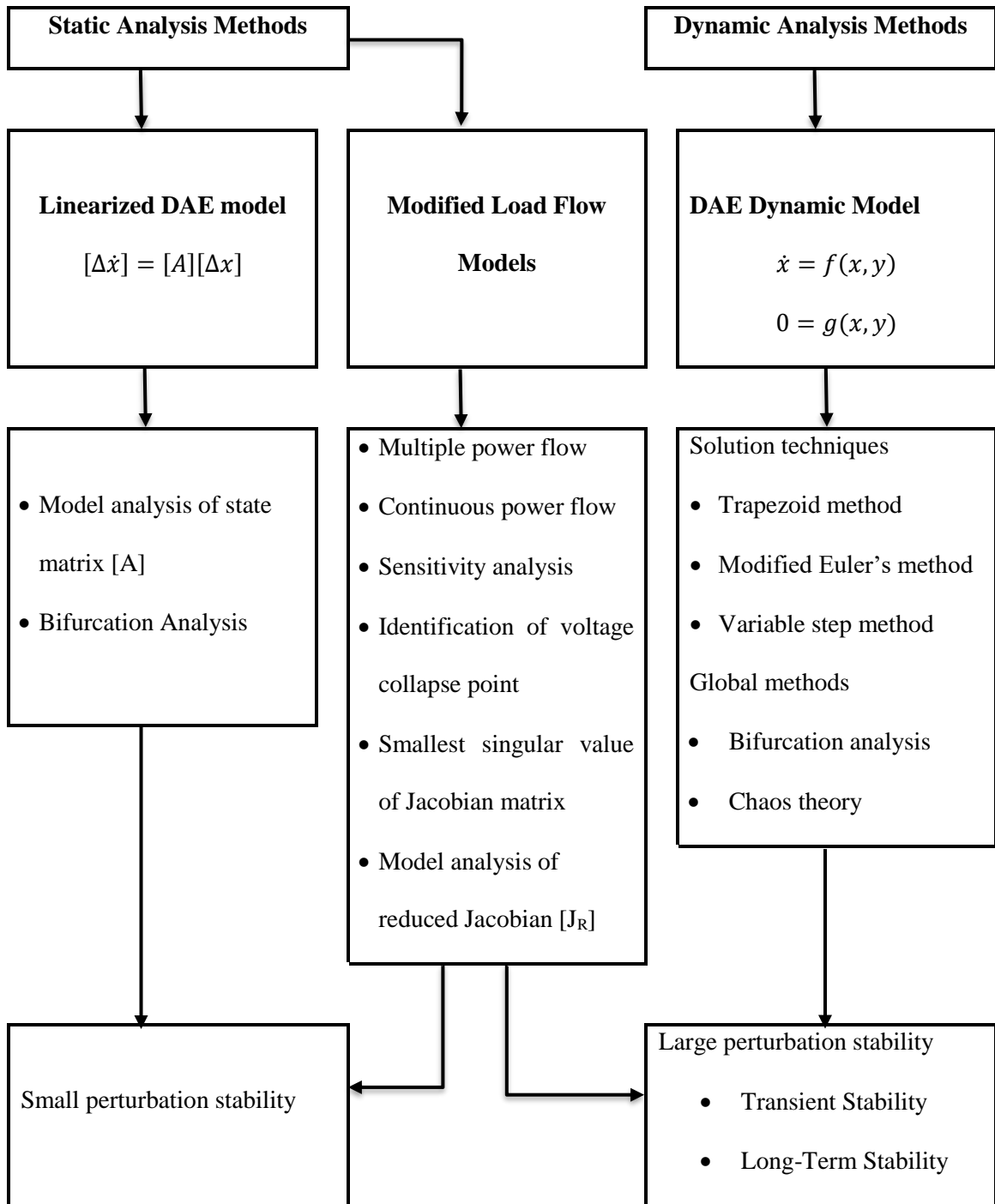- Long-Term Stability

Fig. 2.1 Voltage stability methods in power systems [29].

2.2.1 Static Analysis

A number of methods are implemented for the static analysis of voltage stability as shown in Fig. 2.1. These methods are based either on linearized differential-algebraic equations (DAE) or

on load flow equations. Voltage stability after the small perturbation is obtained through the modal analysis or bifurcation analysis of linearized DAE model. Various static analysis methods like multiple power flow, continuous power flow, sensitivity analysis, etc., utilize load flow equations for stability analysis [29]. The pre-disturbance stable system will maintain its stability only if the bus voltages reach the stable equilibrium after the disturbance. So the power flow equations can be utilized at pre-disturbance and post-disturbance equilibrium conditions. Power flow based static voltage stability methods can be implemented to determine both small perturbation stability and large perturbation stability. Static voltage stability analysis is computationally faster than the dynamic analysis. This is because static stability analysis requires only the solution of algebraic equations while dynamic analysis requires the solution of time domain dynamic equations. Therefore, the power system operators usually depend on the static methods for real-time operation and control of a power system.

2.2.2 Dynamic Analysis

In dynamic analysis, generators, AVRs, turbine-governors and loads are modeled in differential equations while the transmission and distribution network is modeled in terms of algebraic equations. These sets of differential and algebraic equations make a complete mathematical model for dynamic analysis as shown in Fig. 2.1. These equations are solved using one of the numerical solution techniques such as trapezoidal method, modified Euler's method, etc. Dynamic analysis is required for transient and long-term stability when there is large perturbation such as the loss of transmission lines, large loads or generators. Details about the necessity of dynamic analysis for voltage stability is discussed in Chapter V.

2.3 Factors Affecting Voltage Stability

The voltage instability is mainly caused due to the inability of combined transmission and generation system to supply demanded reactive power to the load [26]. This can happen due to

reactive power limits of generators, congestion in transmission lines or due to the dynamic of loads and other devices connected to a power system. Causes of voltage instability are discussed in detail.

2.3.1 Generator reactive power limits

Generators supply a significant amount of reactive power in the power system. When the demanded reactive power of the loads exceeds that produced by compensating devices, the excess reactive power needs to be supplied by generators. Under normal operating conditions, the automatic voltage regulator (AVR) of the generators increase their excitation to supply required reactive power demand and maintains a fixed voltage at the generator buses. The maximum limit of generator active and reactive power is guided by its power capability curve [30]. Then, as the reactive power demand increases beyond the certain limit, the generator's excitation current becomes constant and the generator fails to maintain a fixed voltage at its terminal. This scenario is similar to that the generator act as PQ bus [31]. As a result, the reactive power generated in the system becomes less than the reactive power demanded by the loads, resulting in the decrease in the voltage of the buses, which eventually results into voltage instability.

2.3.2 Reactive Power Compensating Devices

The use of compensating devices has a great advantage in a transmission system. Injection of the reactive power by these devices significantly increases the maximum power capability of the transmission lines and reduces system losses. These compensating devices can also be used as immediate corrective actions to supply demanded reactive power to the load. The capacitor bank is commonly used for shunt compensation as it is inexpensive than other compensating devices. The major disadvantage of this technique is that shunt capacitor generated reactive power depends on the square of the voltage of connected bus. During the voltage instability, with the decrease in bus voltage the reactive power generated by the shunt capacitor decreases [4]. Also, the switching of the capacitor is not very fast. As a result, a capacitor bank cannot maintain good reactive power support during low voltage conditions. To overcome this problem fast switching modern static

reactive power compensating devices are used in the weak buses. Under normal operating conditions, reactive power compensating devices support voltage stability phenomenon. However, due to the use of compensating devices, the transmission network is forced to operate near to maximum capability limit. Therefore, during faulted conditions or during contingencies the system is more prone to voltage instability.

2.3.3   Load Modeling

Various techniques to determine the voltage stability indices depends on the load modeling [7]. Thus, the accuracy of the results obtained from these techniques depends on the accuracy of load modeling. Different static and dynamic load models proposed by several researchers are presented in [13]. The load models used in power systems can be broadly classified into static and dynamic load models. Both types of load models play a significant role in voltage stability. If the system is connected to constant impedance load there will be no stability issue due to loads. The power consumed by constant impedance type of load decreases with the system voltage. The static load that mostly affects voltage stability is a constant power type of load. In this type of load, the total power consumed by the load is constant irrespective of fluctuation in bus voltage. When the voltage of the system decreases due to contingency or fault, the constant power loads draw more current. This additional current drawn from the system increases the system losses and voltage drop in the transmission system, which further decreases the bus voltage. Therefore, this type of static load supports the voltage instability phenomenon[32].

Induction motor loads act as dynamic loads in the power system. A step decrease in the bus voltage causes momentary step reduction in the power. This is followed by the load recovery phenomenon [16]. Reduction of power relieves the stress on the bus-bar for certain time but due to the recovery phenomenon the induction motor behaves as a constant power load and demands more current from the system, forcing the system into the condition of voltage instability. This acts as a fast dynamic load. Thus this type of load also supports the voltage instability phenomenon.

Thermostatic controlled resistance loads are usually used for room heating or space heating purposes. These loads are designed such that it maintains a desired fixed temperature. When the bus voltage decreases, heat generated by the resistive load decreases. So, to maintain constant temperature the on-time of thermostatic load increases. Thus, for long intervals of time, these loads act as exponential recovery load [16] to the system and assist voltage instability.

2.3.4   Underload Tap Changing Transformer (ULTC)

ULTC transformers increase load voltage when the bus-bar voltage decreases. ULTCs are important from the load perspective as it ensures constant voltage across the loads, but these devices impose a negative impact on the system and assist the voltage instability phenomenon. When the voltage of a load bus decreases, a ULTC operates to increase the winding ratio to keep the load voltage constant. This causes the loads to behave as an exponential recovery model eventually increasing the current at the load bus and assisting the voltage instability phenomenon.

2.4   Mechanism of Voltage Instability and Voltage Collapse

Voltage instability is initiated due to small or large disturbances in power systems. Small disturbances are caused due to a slow variation in generation or load and large disturbances are caused due to the outage of transmission lines, transformers, generators, etc. Voltage collapse is usually caused by cascading outage of a number of generators or transmission lines following the disturbances.
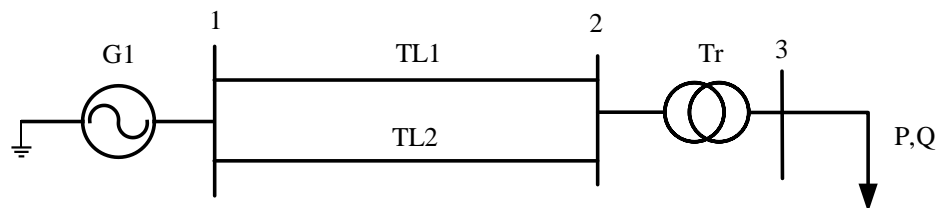
Fig. 2.2 Three bus power system model

13

In Fig. 2.2, generator G1 supply all the power demanded by the load connected at bus 3. TL1 and TL2 are two transmission lines connecting bus 1 and bus 2. A load at bus 3 is supplied through a step-down transformer Tr.

As shown in Fig. 2.3, as the load at bus 3 increases from P1, the voltage of the load bus decreases. When the load demand exceeds the maximum power capability of the transmission line shown by point C, there will be no intersection between PV curve and the load characteristics, which causes the voltage instability and voltage collapse.
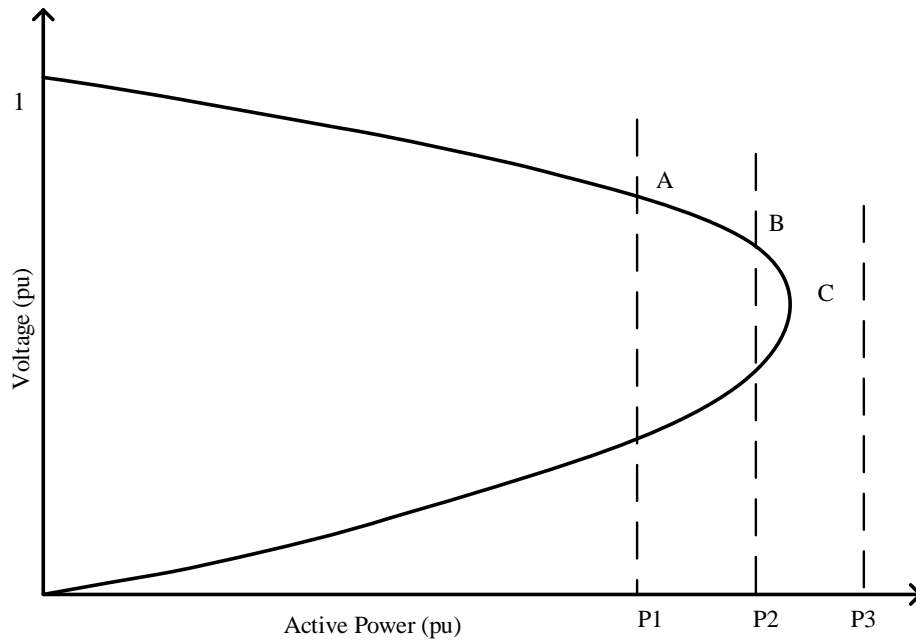
Fig. 2.3. Voltage instability with constant power load

Another mechanism of voltage instability and voltage collapse is large perturbation such as contingency due to the outage of, transmission lines, generators, transformers, etc. In Fig. 2.4, large disturbance causes an outage of TL2. PV1 represents pre-disturbance PV curve and PV2 represents post-disturbance PV curve. It can be observed that load characteristics of P1 intersect with both pre-disturbance and post-disturbance PV curve. So after the contingency, the operating point shifts to A1 and the power system can supply P1 power at reduced voltage. However, load

14

characteristics of P2 do not intersect with post-disturbance PV curve. So, the power system operating at point B results in voltage collapse.
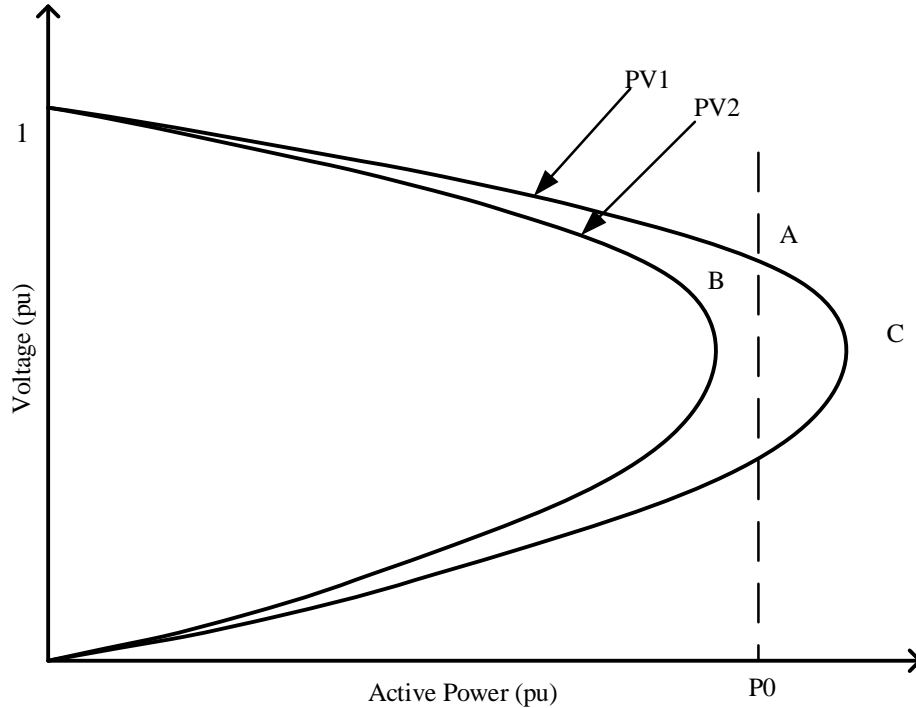
Fig. 2.4. Voltage instability due to contingency with constant power load

2.5   Solutions and Countermeasures for Voltage Instability

As the voltage collapse causes huge economic loss and impacts social life, countermeasures against voltage stability are applied beginning from the design stage to real-time operation of power systems. The power supply should meet the load demand and transmission system should have the capability to transmit the demanded active and reactive power. Power system voltage is strongly linked to reactive power. Supply of reactive power from distant generation sources causes huge transmission line losses, which supports the voltage instability mechanism. A common practice of countermeasure voltage instability is to generate adequate reactive power at the load side. This is usually achieved by installing capacitor banks and modern static reactive power compensating devices, at the planning stage.

For real-time operations, the system operator can have several options to prevent voltage instability. This includes switching capacitor banks, blocking tap changers of transformers, re-dispatching generators, and changing reference voltage at generator buses. If all of these activities fail to restore the system into the normal operating state, the last measure the system operator can take to prevent voltage collapse is load shedding. Although due to load shedding, the people of a certain area will be deprived of electricity for a certain time this can prevent voltage collapse.
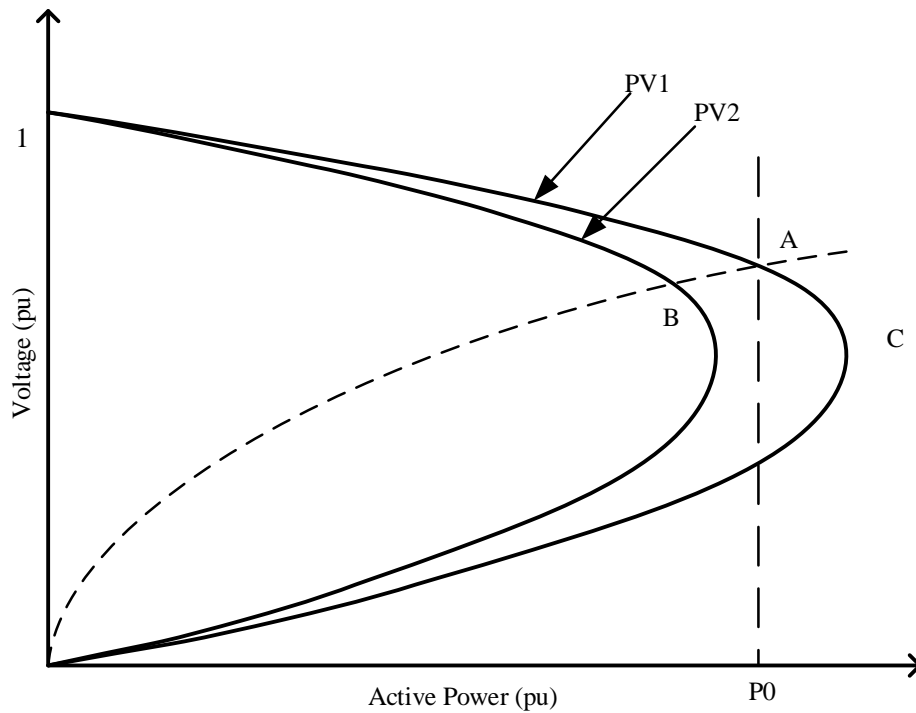
Fig. 2.5. Impact of load modeling on voltage stability.

Voltage stability also depends on the type of connected loads. In Fig. 2.5, pre-disturbance and post-disturbance PV curve is shown with constant power and constant impedance load characteristics. In pre-disturbance condition, both types of load consume P0 power at the same voltage which can be obtained from operating point A. However, constant power load characteristics do not intersect while the constant impedance load characteristics intersect with the post-disturbance PV curve. Thus, the load characteristics make a significant difference in voltage

stability which can be utilized as a countermeasure for voltage instability. As a demand-side management, the constant power load can be converted into constant impedance type of load using the Point of Load Converter (POLC) [33], which can have a significant impact in voltage stability.

CHAPTER III

MODELING OF POWER SYSTEM DEVICES FOR VOLTAGE STABILITY ANALYSIS

The fundamental step for simulation and analysis of the power system is the modeling of all the connected components in the system. The generators, loads and all other connected devices must be modeled for static and dynamic analysis. For static analysis of power system, one generator connected to swing bus is modeled as a voltage source with fixed terminal voltage and capable of producing any amount of active and reactive power demanded by the system. All other generators are modeled as sources, which produce fixed active power keeping its terminal voltage constant. Loads are modeled as constant power loads, constant impedance loads, constant current loads, or any combination of these loads.

The static analysis for voltage stability based on power flow equations is applied when the system is in equilibrium state before or after any disturbances. These static methods are used to know the state of the power system and to ensure that it is operating with suitable margin form the point of maximum loadability. However, these static analysis methods with the above-mentioned modeling do not capture the detail dynamics of voltage instability mechanism. This requires time domain analysis. The generators and other devices connected to the power systems are modeled in terms of differential and algebraic equations for time domain analysis. Detail modeling of synchronous generators, excitation system, governor system and load models are described in subsequent sections.

3.1   Synchronous Generator Modeling

One of the major components of the power system is a synchronous generator. A number of synchronous generator models are developed in which generators are expressed as transient or sub-transient emf behind appropriate reactance. Generator equivalent circuit neglecting resistance is shown in Fig 3.1.
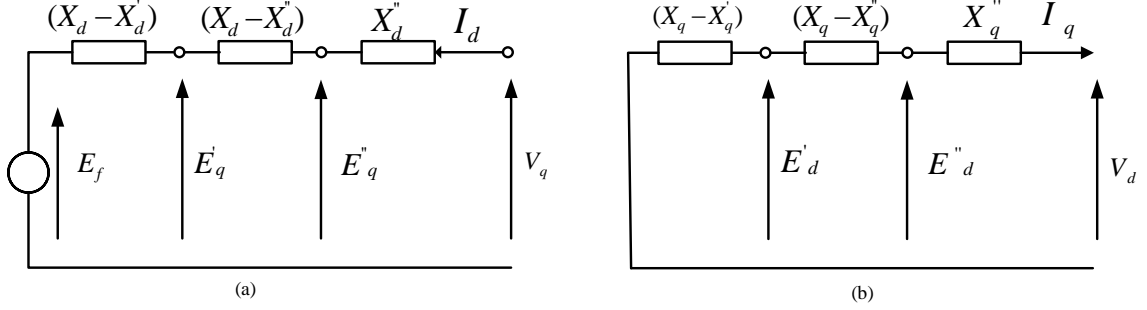
Fig. 3.1. Equivalent circuit for synchronous generator: (a) d-axis; (b) q-axis [34]

In this research work, generators are modeled as sixth order generator model, which consists of six differential equations. In this model, generator is expressed as sub-transient emf E_q'' and E_d'' behind subtransient reactance X_d'' and X_q'' respectively. The set of six differential equations are given in (3.1)-(3.6). P_m is obtained form turbine and governor system model and E_f is calculated form excitation system. The air gap power of synchronous generator is obtained as in (3.7). The terminal voltage of synchronous machine is obtained form (3.8) [33].

$$M\Delta\dot{\omega} = P_m - P_e \tag{3.1}$$

$$\dot{\delta} = \Delta\omega \tag{3.2}$$

$$T_{do}'\dot{E}_q' = E_f - E_q' + I_d(X_d - X_d') \tag{3.3}$$

$$T_{qo}'\dot{E}_d' = -E_d - I_q(X_q - X_q') \tag{3.4}$$

$$T_{do}''\dot{E}_q'' = E_q' - E_q'' + I_d(X_d' - X_d'') \tag{3.5}$$

$$T_{qo}''\dot{E}_d'' = E_d' - E_d'' - I_q(X_q' - X_q'') \tag{3.6}$$

$$P_e = (E_d''I_d + E_q''I_q) + (X_d'' - X_q'')I_qI_d \tag{3.7}$$

19

$$\begin{bmatrix} V_d \\ V_q \end{bmatrix} = \begin{bmatrix} E_d'' \\ E_q'' \end{bmatrix} - \begin{bmatrix} R & X_q'' \\ X_d'' & R \end{bmatrix} \begin{bmatrix} I_d \\ I_q \end{bmatrix} \tag{3.8}$$

3.2   Excitation System Modeling

Excitation system plays a major role in reactive power support and voltage stability. The major components of excitation system are exciter, voltage regulator, power system stabilizer, over-excitation limiters, terminal voltage transducers, and load compensators. The function of each component is described.

- **Exciter:** It produces the required DC voltage which can be injected into the field winding of synchronous generator. Voltage source should be such that its output voltage can be quickly changed as desired.

- **Voltage Regulator:** Generator terminal voltage is fed to the voltage regulator which produces the error signal based on the desired terminal voltage. The error signal is fed to exciter which acts to change the excitation current. Thus voltage regulator maintains a constant voltage at the generator terminal.

- **Terminal Voltage Transducer:** It senses terminal voltage which is rectified, filtered into dc voltage and compared it with the desired terminal voltage. The error signal is sent to the regulator.

- **Power System Stabilizer:** It is also the component of excitation control system which acts to decrease the power system oscillations. It takes speed deviation, frequency deviation and accelerating power as the input.

- **Over-Excitation Limiters:** This is one of the components of limiters and protective circuit block in excitation system. The major function of the over-excitation limiter is to limit the excitation current when the generator's field current exceeds the certain value for more than certain period of time. The maximum value of the field current is based on the field winding thermal capacity.
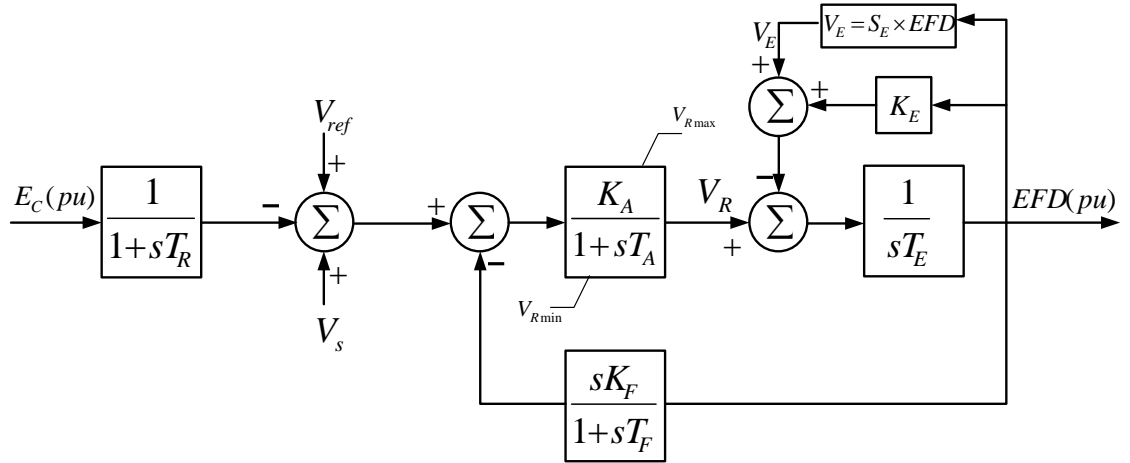
Fig. 3.2   Excitation System [26]

There are various modes of excitation system implemented, in this thesis work IEEET1 model of PSS/E is used. Block diagram of an excitation system is shown in Fig. 3.2.

3.3   Governor System Modeling
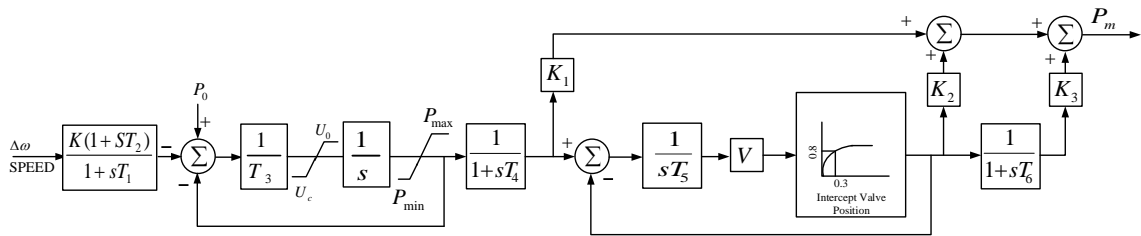
Fig. 3.3 Governor System [35]

The power system load is not constant. To meet the changing load demands all the times and to maintain power system stability, governor system is essential. Governor constantly monitors the speed of the shaft of the generator and based on its speed, it operates to change the mechanical input to the generator. Mechanical power is increased for the shaft speed less than synchronous speed and the mechanical power is decreased for the shaft speed more than the synchronous speed. The modeling of the governor is specific to the type of turbine-governor system. This thesis work uses steam turbine driven generator and the governor used in this work is TGOV3 model of PSS\E. Block diagram of a governor system is shown in Fig. 3.2.

3.4   Load Modeling

.   The load models used in power systems are broadly classified into static and dynamic load models. Static and dynamic load models are described in subsequent sections.

3.4.1   Static Load Models

The power consumed by static load models doesn't depend on time. Commonly used static load models are an exponential model and ZIP model [26].

$$P = P_0 \left[\left(\frac{v}{v_0} \right)^{kp} \right] \tag{3.9}$$

$$Q = Q_0 \left[\left(\frac{v}{v_0} \right)^{kq} \right] \tag{3.10}$$

In exponential load model, the active and reactive power consumed by loads are represented as a function of bus voltage. Power consumed by the load depends on load characteristics which are a function of bus voltage. When the bus voltage is equal to the reference voltage v_0, load consumes P_0 active power and Q_0 reactive power. The active and reactive power consumption depends on bus voltage and the value of kp and kq.

$$P = P_0 \left[a_1 \left(\frac{v}{v_0} \right)^2 + a_2 \left(\frac{v}{v_0} \right)^1 + a_3 \left(\frac{v}{v_0} \right)^0 \right] \tag{3.11}$$

$$Q = Q_0 \left[b_1 \left(\frac{v}{v_0} \right)^2 + b_2 \left(\frac{v}{v_0} \right)^1 + b_3 \left(\frac{v}{v_0} \right)^0 \right] \tag{3.12}$$

ZIP model is the combination of constant power load, constant admittance loads and constant current load. The active and reactive power consumed by the load is given as (3.11) and (3.12).

If the system is connected to only constant impedance type of loads there will be no voltage stability issue in the system. The power consumed by constant impedance type of load decreases

with a decrease in system voltage. The static load that mostly affects voltage stability is a constant power type of load.

3.4.2 Dynamic Load Models

Industries used static load models to analyze the power systems before 1980's [36]. For several faults, the system did not restore to normal voltage long time after the faults were cleared. Also, the voltage oscillations were observed for an extended period of time. It was realized that these dynamics were attributed to the motor loads connected to the system which was not observed when the system was simulated using static load models. Also, the type of loads connected to the system is changed and the load contribution of air-conditioners are increased. Due to the inability of static loads to represent true load dynamics and to address changing load pattern, it was realized that the load models should represent major types of loads connected to the system. Thus, complex load model was developed which includes motor loads, discharge lighting loads, static loads and polynomial loads.

$$P + jQ$$

$$\frac{R + jX}{P_0}$$

M — Large Motors

M — Small Motors

I / V — Discharge Lighting

I / V — Transformer Saturation

Constant MVA

$$P = P_R \times V^{K_P}$$
$$Q = Q_R \times V^2$$

Remaining Loads
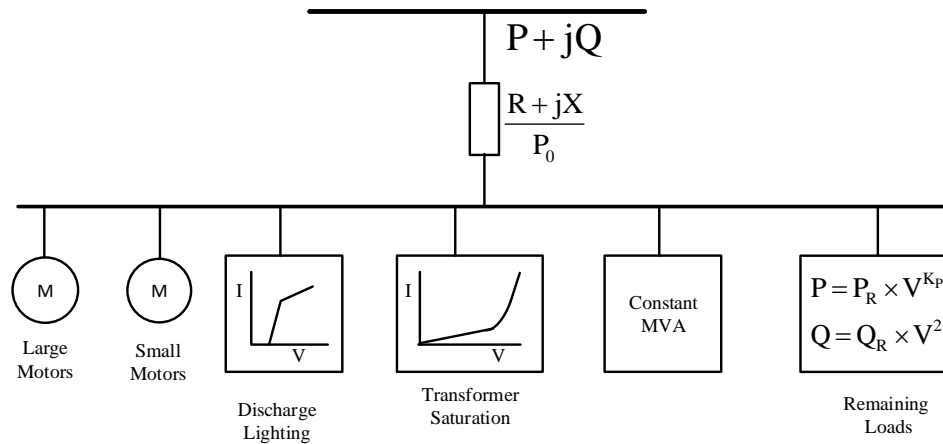
Fig. 3.4. Complex load model [37].

In the complex load model given in Fig. 3.4, motor loads are modeled as an equivalent circuit shown in Fig. 3.5. The corresponding values of parameters of an equivalent circuit for large motors and small motors are given in Table 3.1 and Table 3.2.

23
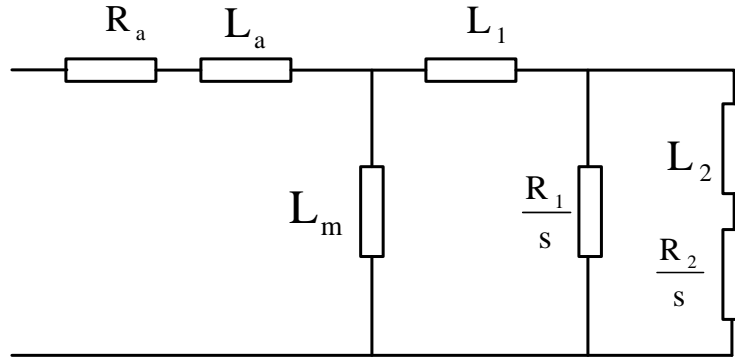
Fig. 3.5. Circuit Diagram for Induction Motor

Table 3.1. Circuit parameters for large induction motor

R_a	L_a	L_m	R_1	L_1	R_2	L_2	H	Initial Slip
0.0138	0.0830	3.00	0.055	0.053	0.0115	0.055	1	-0.00837

Table 3.2 Circuit parameters for small induction motor

R_a	L_a	L_m	R_1	L_1	R_2	L_2	H	Initial Slip
0.0369	0.1318	2.396	0.0645	0.0415	0.0489	0.3210	0.6	-0.02149

CHAPTER IV

STATIC VOLTAGE STABILITY ANALYSIS

Static voltage stability analysis is based on power flow solutions. Static voltage stability depends on the power transfer capability of the transmission system. This power transfer capability can be determined through power flow solutions. In power flow analysis, it is assumed that the generated power is equal to the sum of power consumed and system losses. The system is assumed to be in perfect equilibrium, with a constant frequency. Active and reactive power of each bus is formulated in terms of nodal admittance and bus voltages in phasor form. The nonlinear equations thus obtained are solved using Newton-Raphson (N-R) method. In the following sections, formulation of power flow equations and power flow solution using N-R method are presented. Thereafter, power flow solution based static voltage stability analysis is discussed in detail.

4.1   Power Flow Formulation

Consider n bus power system, linear relation of current and voltage in each bus in matrix form is given in (4.1).

$$\boldsymbol{I} = \boldsymbol{YV} \tag{4.1}$$

Where,

$$I = \begin{bmatrix} I_1 \\ I_2 \\ . \\ . \\ . \\ . \\ I_n \end{bmatrix}, V = \begin{bmatrix} V_1 \\ V_2 \\ . \\ . \\ . \\ . \\ V_n \end{bmatrix}$$

$$Y = \begin{bmatrix} Y_{11} & Y_{12} & . & . & . & Y_{1n} \\ Y_{21} & Y_{21} & . & . & . & Y_{2n} \\ ... & ... & . & . & . & ... \\ Y_{n1} & Y_{n2} & . & . & . & Y_{nn} \end{bmatrix}$$

I is the net injected bus current vector, **Y** is bus admittance matrix and **V** is the bus voltage vector and.

From (4.1) the injected current at bus i is given in (4.2).

$$I_i = \sum_{j=1}^{n} Y_{ij}V_j \tag{4.2}$$

Equation (4.2) can be written in polar form as [38]

$$I_i = \sum_{j=1}^{n} |Y_{ij}||V_j| \angle \theta_{ij} + \delta_j \tag{4.3}$$

For the formulation of power flow problem, active and reactive power in terms of injected current is expressed as

$$P_i + jQ_i = V_i I_i^*$$

Or,

$$P_i - jQ_i = V_i^* I_i \tag{4.4}$$

From (4.3) and (4.4) we get,

$$P_i - jQ_i = |V_i| \angle -\delta_i \sum_{j=1}^{n} |Y_{ij}||V_j| \angle \theta_{ij} + \delta_j \tag{4.5}$$

Equating real and imaginary parts we get,

$$P_i = \sum_{j=1}^{n} |V_i||V_j||Y_{ij}| \cos(\theta_{ij} - \delta_i + \delta_j) \tag{4.6}$$

$$Q_i = -\sum_{j=1}^{n} |V_i||V_j||Y_{ij}| \sin(\theta_{ij} - \delta_i + \delta_j) \tag{4.7}$$

4.2   Newton-Raphson Method

Newton-Raphson (N-R) method is one of the most widely used technique to solve nonlinear power flow equations [39]. To illustrate the concept of N-R method, let us consider n nonlinear equations with n variables.

$$f_1(x_1, x_2, x_3, \ldots \ldots x_n) = a_1$$

$$f_2(x_1, x_2, x_3, \ldots \ldots x_n) = a_2$$

$$f_3(x_1, x_2, x_3, \ldots \ldots x_n) = a_3 \tag{4.8}$$

$$\ldots \ldots \ldots \ldots \ldots \ldots \ldots \ldots \ldots \ldots$$

$$f_n(x_1, x_2, x_3, \ldots \ldots x_n) = a_n$$

Let $x_1^0, x_2^0, x_3^0, \ldots x_n^0$ are initial estimate solutions for (4.8) and $\Delta x_1{}^0 \, \Delta x_2{}^0 \, \Delta x_3{}^0 \ldots \Delta x_n{}^0$ be deviation of estimate solutions from accurate solutions. Equation (4.8) becomes,

$$f_1(x_1^0 + \Delta x_1{}^0, x_2^0 + \Delta x_2{}^0, x_3^0 + \Delta x_3{}^0, \ldots \ldots x_n^0 + \Delta x_n{}^0) = a_1$$

$$f_2(x_1^0 + \Delta x_1{}^0, x_2^0 + \Delta x_2{}^0, x_3^0 + \Delta x_3{}^0, \ldots \ldots x_n^0 + \Delta x_n{}^0) = a_2$$

$$f_3(x_1^0 + \Delta x_1{}^0, x_2^0 + \Delta x_2{}^0, x_3^0 + \Delta x_3{}^0, \ldots \ldots x_n^0 + \Delta x_n{}^0) = a_3 \tag{4.9}$$

$$\ldots \ldots \ldots \ldots \ldots \ldots \ldots \ldots \ldots \ldots \ldots \ldots \ldots \ldots \ldots \ldots \ldots$$

$$f_n(x_1^0 + \Delta x_1{}^0, x_2^0 + \Delta x_2{}^0, x_3^0 + \Delta x_3{}^0, \ldots \ldots x_n^0 + \Delta x_n{}^0) = a_n$$

Equations (4.9) is expanded using Taylor series about initial estimate solutions. Assuming deviations from initial estimate very small, higher order terms are ignored.

$$f_i(x_1^0 + \Delta x_1{}^0, x_2^0 + \Delta x_2{}^0, x_3^0 + \Delta x_3{}^0, \ldots \ldots x_n^0 + \Delta x_n{}^0)$$

$$= f_i{}^0 + \left(\frac{\partial f_i}{\partial x_1}\right) \Delta x_1{}^0 + \left(\frac{\partial f_i}{\partial x_2}\right) \Delta x_2{}^0 + \cdots \left(\frac{\partial f_i}{\partial x_n}\right) \Delta x_n{}^0 \tag{4.10}$$

Where,

$$f_i{}^0 = f_i(x_1^0, x_2^0, x_3^0, \ldots \ldots x_n^0)$$

After Taylor series expansion of (4.9), the resulting equations are written in matrix form as [38]

$$
\begin{bmatrix} a_1 - f_1{}^0 \\ a_2 - f_2{}^0 \\ . \\ . \\ . \\ a_n - f_n{}^0 \end{bmatrix} =
\begin{bmatrix}
\left(\frac{\partial f_1}{\partial x_1}\right)^0 & \left(\frac{\partial f_1}{\partial x_2}\right)^0 & \cdots\cdots\cdots & \left(\frac{\partial f_1}{\partial x_n}\right)^0 \\
\left(\frac{\partial f_2}{\partial x_1}\right)^0 & \left(\frac{\partial f_2}{\partial x_2}\right)^0 & \cdots\cdots\cdots & \left(\frac{\partial f_2}{\partial x_n}\right)^0 \\
\cdots\cdots\cdots\cdots\cdots\cdots\cdots\cdots\cdots\cdots\cdots\cdots\cdots \\
\left(\frac{\partial f_n}{\partial x_1}\right)^0 & \left(\frac{\partial f_n}{\partial x_2}\right)^0 & \cdots\cdots\cdots & \left(\frac{\partial f_n}{\partial x_n}\right)^0
\end{bmatrix}
\begin{bmatrix} \Delta x_1{}^0 \\ \Delta x_2{}^0 \\ . \\ \Delta x_n{}^0 \end{bmatrix}
\tag{4.11}
$$

Matrix equation (4.11) can be written as

$$\Delta A^k = J^k \Delta X^k \tag{4.12}$$

Equation (4.12) can be written as

$$\Delta X^k = [J^k]^{-1} \Delta A^k \tag{4.13}$$

Where,

$$
\Delta X^k = \begin{bmatrix} \Delta x_1{}^k \\ \Delta x_2{}^k \\ . \\ . \\ \Delta x_n{}^k \end{bmatrix},\ \Delta A^k = \begin{bmatrix} a_1 - f_1{}^k \\ a_2 - f_2{}^k \\ . \\ . \\ . \\ a_n - f_n{}^k \end{bmatrix}
\qquad
J^k = \begin{bmatrix}
\left(\frac{\partial f_1}{\partial x_1}\right)^k & \left(\frac{\partial f_1}{\partial x_2}\right)^k & \cdots\cdots\cdots & \left(\frac{\partial f_1}{\partial x_n}\right)^k \\
\left(\frac{\partial f_2}{\partial x_1}\right)^k & \left(\frac{\partial f_2}{\partial x_2}\right)^k & \cdots\cdots\cdots & \left(\frac{\partial f_2}{\partial x_n}\right)^k \\
\cdots\cdots\cdots\cdots\cdots\cdots\cdots\cdots\cdots\cdots\cdots\cdots \\
\left(\frac{\partial f_n}{\partial x_1}\right)^k & \left(\frac{\partial f_n}{\partial x_2}\right)^k & \cdots\cdots\cdots & \left(\frac{\partial f_n}{\partial x_n}\right)^k
\end{bmatrix}
$$

$$X^{(k+1)} = X^{(k)} + \Delta X^{(k)} \tag{4.14}$$

J^k is Jacobian matrix. ΔA^k is error matrix, which is the difference of actual value and calculated value of nonlinear equations. ΔX^k is the correction vector obtained from (4.13). Starting from initial guess, solution of equations in each iteration is obtained from (4.14). Final solution is obtained when the mismatch vector $\Delta X^{(k)}$ is sufficiently small.

4.3   Power Flow Solution with Newton-Raphson Method

Steady state power system is represented by (4.6) and (4.7) for each bus. The number of equations required for load flow solution depends on the type of power system buses. In general, Power system buses are classified into slack bus, generator bus, and load bus

- Load bus (PQ bus): It is the node in power system in which loads are connected. In power flow analysis, loads are considered as constant power load represented by active power (P) and reactive power (Q). In this bus, P and Q are known while magnitude and phase of load bus are obtained from power flow solution.

- Generator bus (PV bus): The nodes in which the power generators are connected are called as generator buses. In generator buses, the active power injection and voltage magnitude (V) of generator bus are known. Voltage angle (δ) and Q are determined through power flow solution.

- Slack bus (AV bus): Voltage magnitude and angle of this bus are known while P and Q of the bus are determined through load flow solution. The slack bus is responsible to supply any mismatch power in the system.

Consider a n bus power system with ng number of generators connected to it. Bus 1 is considered as slack bus. For load flow solution, we have active power equation (4.6) for each generator bus and both active and reactive power equation (4.6) and (4.7) for each load buses. Nonlinear power flow equations are solved with N-R method as explained in section 4.2. All four parameters of each bus are determined through load flow solution.

$$P_i = \sum_{j=1}^{n} |V_i||V_j||Y_{ij}| \cos(\theta_{ij} - \delta_i + \delta_j) \qquad (i = 2,3 \dots \dots n) \qquad (4.15)$$

$$Q_i = -\sum_{j=1}^{n} |V_i||V_j||Y_{ij}| \sin(\theta_{ij} - \delta_i + \delta_j) \quad (i = ng + 1, ng + 2 \dots \dots n) \quad (4.16)$$

$$
\begin{bmatrix} \Delta P_2^{(k)} \\ \cdot \\ \cdot \\ \cdot \\ \Delta P_n^{(k)} \\ \hline \Delta Q_{ng+1}^{(k)} \\ \cdot \\ \cdot \\ \cdot \\ \Delta Q_n^{(k)} \end{bmatrix} = \left[\begin{array}{ccc|ccc} \dfrac{\partial P_2}{\partial \delta_2}^{(k)} & \cdots & \dfrac{\partial P_2}{\partial \delta_n}^{(k)} & \dfrac{\partial P_2}{\partial V_{ng+1}}^{(k)} & \cdots & \dfrac{\partial P_2}{\partial V_n}^{(k)} \\ \vdots & \ddots & \vdots & \vdots & \ddots & \vdots \\ \dfrac{\partial P_n}{\partial \delta_2}^{(k)} & \cdots & \dfrac{\partial P_n}{\partial \delta_n}^{(k)} & \dfrac{\partial P_n}{\partial V_{ng+1}}^{(k)} & \cdots & \dfrac{\partial P_2}{\partial V_n}^{(k)} \\ \hline \dfrac{\partial Q_{ng+1}}{\partial \delta_2}^{(k)} & \cdots & \dfrac{\partial Q_{ng+1}}{\partial \delta_n}^{(k)} & \dfrac{\partial Q_{ng+1}}{\partial V_{ng+1}}^{(k)} & \cdots & \dfrac{\partial Q_{ng+1}}{\partial V_n}^{(k)} \\ \vdots & \ddots & \vdots & \vdots & \ddots & \vdots \\ \dfrac{\partial Q_n}{\partial \delta_2}^{(k)} & \cdots & \dfrac{\partial Q_n}{\partial \delta_n}^{(k)} & \dfrac{\partial Q_n}{\partial V_{ng+1}}^{(k)} & \cdots & \dfrac{\partial Q_n}{\partial V_n}^{(k)} \end{array} \right] \begin{bmatrix} \Delta \delta_2^{(k)} \\ \cdot \\ \cdot \\ \cdot \\ \Delta \delta_n^{(k)} \\ \hline \Delta V_{ng+1}^{(k)} \\ \cdot \\ \cdot \\ \cdot \\ \Delta V_n^{(k)} \end{bmatrix}
\tag{4.17}
$$

Linearized load flow equation (4.17) can be written as [26]

$$
\begin{bmatrix} \Delta P \\ \Delta Q \end{bmatrix} = \begin{bmatrix} J_{P\delta} & J_{PV} \\ J_{Q\delta} & J_{QV} \end{bmatrix} \begin{bmatrix} \Delta \delta \\ \Delta V \end{bmatrix}
\tag{4.18}
$$

Where,

$$
\Delta P_i^{(k)} = P_i^{(sch)} - P_i^{(cal)}
\tag{4.19}
$$

$$
\Delta Q_i^{(k)} = Q_i^{(sch)} - Q_i^{(cal)}
\tag{4.20}
$$

$\Delta P_i^{(k)}$ and $\Delta Q_i^{(k)}$ are power mismatch at k^{th} iteration, which are the difference of scheduled power and calculated power at k^{th} iteration. Voltage angle and magnitude of ith bus at k^{th} iteration are obtained from (4.21) and (4.22)

$$
\delta_i^{(k+1)} = \delta_i^{(k)} + \Delta \delta_i^{(k)}
\tag{4.21}
$$

$$
V_i^{(k+1)} = V_i^{(k)} + \Delta V_i^{(k)}
\tag{4.22}
$$

4.4   Techniques for Static Voltage Stability Analysis

A power system is modeled with a set of equations (4.6), (4.7) and (4.23), called the Differential-Algebraic Equations [40].

$$
\dot{x} = f(x, V)
\tag{4.23}
$$

Where, V is bus voltage vector and x is state vector which is related to the dynamics of generator, loads and other devices connected to power system. For static analysis, all types of generator and

load dynamics are ignored and power system is simply represented by nonlinear algebraic equations (4.6) and (4.7). Techniques for static voltage stability are based on static power flow equations [28]. The static voltage stability analysis presented in this thesis are based on the analysis of PV curves and QV curves.

4.5   Concept Explanation for PV Curves.

PV curve is the graph obtained by plotting the bus voltage against the power supplied to the load. Maximum loadability is the corresponding power value at the nose point of PV curve [17]. The maximum power that can be transferred to loads depends on the availability of generated power, power transfer capability of the transmission line and the load power factor. Various methods are implemented to determine maximum power transfer capability of a power system. For the steady-state analysis, it is assumed that the generators are capable of producing sufficient active and reactive power. Then, the maximum loadability depends on the transmission lines and power factor of the load.

Consider a two bus system with a load connected to a generator through the transmission line. The generator is modeled such that it can supply any amount of power demanded with constant terminal voltage. The value of a load connected to bus 2 is continuously increased and the voltage at the load bus is obtained through power flow calculations.
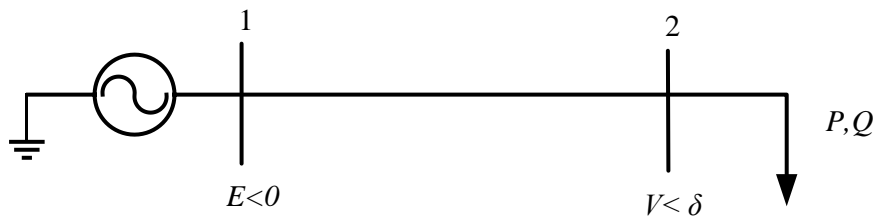

Fig. 4.1 Two bus power system

The active and reactive power consumed by the load is given by (4.24) and (4.25)

$$P = \frac{-V\mathrm{E}}{\mathrm{X}}\ sin\delta \tag{4.24}$$

$$Q = \frac{VE}{X} cos\delta - \frac{V^2}{X} \tag{4.25}$$

Solving (4.24) and (4.25) for voltage, we get the following expressions [27].

$$V = \sqrt{\frac{E^2 - 2QX + \sqrt{E^4 - 4X^2P^2 - 4XE^2Q}}{2}} \tag{4.26}$$

$$V = \sqrt{\frac{E^2 - 2QX - \sqrt{E^4 - 4X^2P^2 - 4XE^2Q}}{2}} \tag{4.27}$$

To obtain a PV curve, the load power factor is kept constant. P and Q are increased and the corresponding value of voltage is obtained from (4.26) and (4.27). Voltage is plotted against corresponding power and PV curve is obtained as shown in Fig. 4.2. In a simple two bus power system, power flow equations (4.24) and (4.25) can be analytically solved to get the expression for voltage in terms of the connected load.
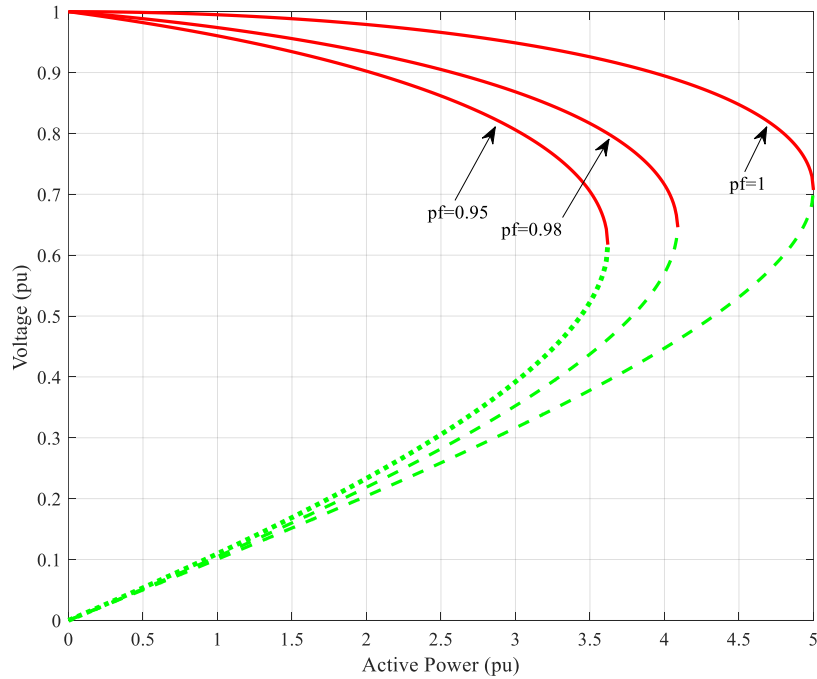

Fig. 4.2. PV curve for two bus system

From PV curve it can be observed that, for a single value of the active load, there can be two possible voltage values. Equation (4.26) gives high voltage solutions shown by solid lines, while (4.27) gives low voltage solutions for same value load shown by dashed lines in Fig. 4.2. The high voltage and low voltage solutions intersect at a point which represents the maximum loadability of the system. Voltage collapse is inevitable if the system is subjected to load beyond the maximum loading point. Ignoring all types of dynamics, the power system can theoretically operate at any point in PV curve. The practical power system is not a static system as it is subjected to various disturbances on the load side, generation side or in the transmission system. These dynamics perturb the system from equilibrium. At such situation, the power system can regain its equilibrium state and continue to operate only if the operating point is above the maximum loading point. However, voltage collapse occurs if the operating point is below the maximum loading point. Thus, PV curve gives important information for the power system operator regarding the stable operating point of a system. Additionally, through PV curve, the system operator can get an idea about the additional load of the system which can handle without losing its stability.

4.6   Power System Model for Static Analysis

The test system is shown in Fig. 4.3 will be used for static voltage stability analysis. The required data is given in Appendix. IEEE 9 bus system consists of three loads connected at three buses and the power demanded by the load is supplied by three generators connected to the system. For the purpose of static analysis, it is assumed that generators G2 and G3 produces fixed active power and maintains fixed terminal voltage. Generator G1 maintains fixed terminal voltage and produces the mismatch power as it is connected to the slack bus. Matpower is used to obtain results for static analysis in this thesis. Matpower is a group of Matlab m-files which are mainly used for power flow analysis [41].
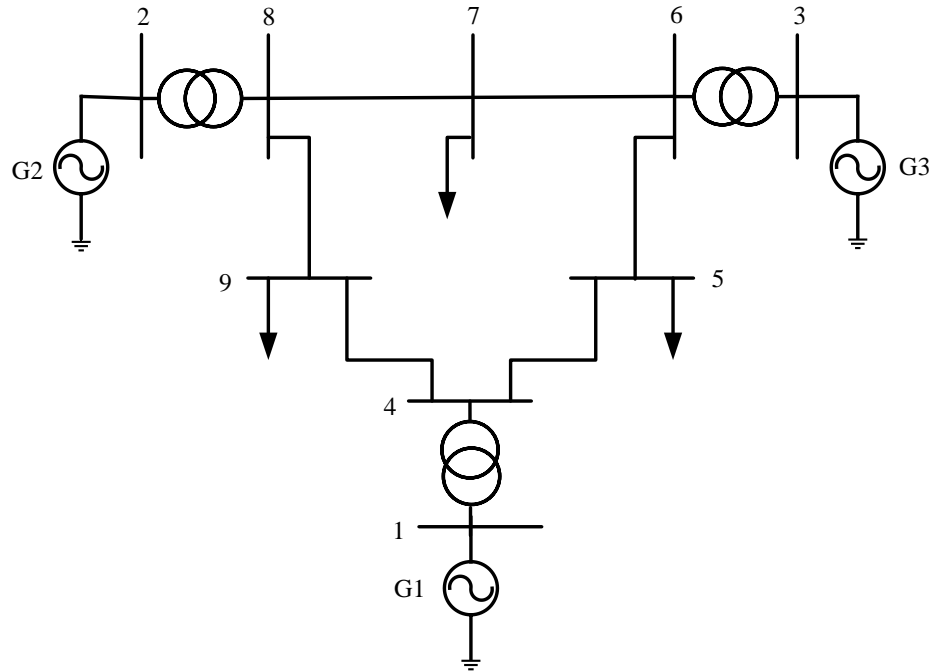
Fig. 4.3. IEEE 9 bus system for static voltage stability analysis.

4.7   PV Curve with Multiple Load-Flow Method

In this method, the PV curve is obtained through multiple load flow solutions and power flow solution is obtained using the N-R method, as described in section 4.3. First, the power flow solution for the no-load case is obtained and the process is repeated with increased load and generation until N-R method produces converged solutions. At each iteration, the value of connected loads as well as source is increased by one percent of base case load. Multiple load flow method for PV curve is implemented for IEEE 9 bus system shown in Fig. 4.3.

PV curve for bus 9 obtained using multiple power flow method is shown in Fig 4.4. It illustrates that the maximum power transfer limit increases with increase in power factor (pf) of the load. Additionally, it is observed that the minimum stable voltage increases with increase in power factor. At bus 9 of IEEE 9 bus system, 0.7 p.u is the minimum voltage with unity power factor while the minimum stable voltage decreases to 0.61 p.u when pf is 0.93.
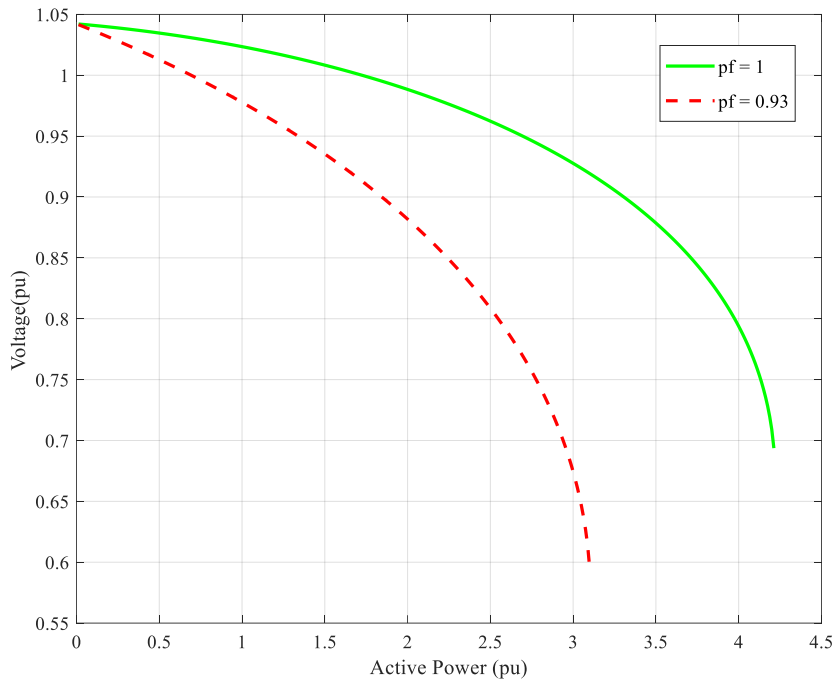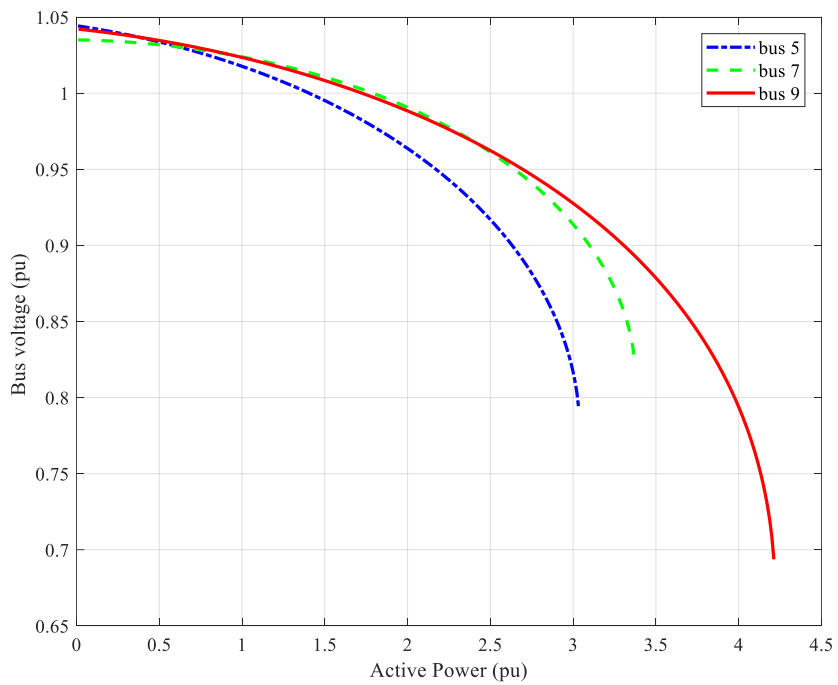
34

Fig. 4.4. PV curve for bus 9

Fig. 4.5. PV curve for load buses at unity pf load

The Fig. 4.5 shows the PV curve of all the load buses at unity pf. The minimum stable voltage of the system is 0.68 p.u for bus 9. From the figure, it can be deduced that bus 7 can have 0.7 p.u before it goes to instability while the system goes to instability if bus voltage at bus 5 and bus 7 is less than 0.79 p.u and 0.83 p.u respectively. Therefore, the stability of the system cannot be determined by the absolute value of bus voltage.

4.8   Continuous Power Flow Method

Newton-Raphson method fails to converge near maximum power transfer point due to the singularity of Jacobian matrix [42]. This problem can be avoided by the use of continuous power flow (CPF) method [6]. The first step of this method is that the power flow solution is obtained through normal load flow method at base load. Then, the next solution of the load flow is obtained through the predictor and corrector process. In the predictor process, the tangent vector is obtained with appropriately sized step and the corrector equation is obtained by the use of parameterization technique [43]. The CPF method uses local parameterization technique. In this method, load parameter λ is taken as a continuous parameter and the value of this parameter is continuously updated. The value of λ is zero at base load and it increases to λ_{cr} at the critical point (maximum loading). The value of $d\lambda$ is positive until the critical point is reached, then its value becomes negative. The critical point will be determined by sensing the value of $d\lambda$. Power flow equations can be written in the form of nonlinear equations

$$F(\delta, V) = 0 \tag{4.28}$$

In CPF method, load parameter λ is introduced and the nonlinear equations are written as

$$F(\delta, V, \lambda) = 0 \tag{4.29}$$

For CPF, the generated power and the load equations are modified as [6]

$$P_l(\lambda) = P_{lo}(1 + \lambda K_l) \tag{4.30}$$

$$Q_l(\lambda) = Q_{lo}(1 + \lambda K_l) \tag{4.31}$$

$$P_G(\lambda) = P_{Go}(1 + \lambda K_G) \tag{4.32}$$

Where, P_{lo} is active power of the base load, Q_{lo} is reactive power of the base load, P_{Go} is active power generated at base case, K_l is rate of change of load, K_G is rate of change of generation and λ is continuation parameter. Thus, continuous load flow equations are formulated as in (4.30) - (4.32). For predictor process, (4.33) is solved and the predicted solution is obtained from (4.34)

$$\begin{bmatrix} F\delta & Fv & F\lambda \\ & ek & \end{bmatrix} \begin{bmatrix} d\delta \\ dv \\ d\lambda \end{bmatrix} = \begin{bmatrix} 0 \\ \pm 1 \end{bmatrix} \tag{4.33}$$

$$\begin{bmatrix} \delta^* \\ V^* \\ \lambda^* \end{bmatrix} = \begin{bmatrix} \delta \\ v \\ \lambda \end{bmatrix} + \sigma \begin{bmatrix} d\delta \\ dv \\ d\lambda \end{bmatrix} \tag{4.34}$$

Where, σ is the step length and ek is a row vector. In the corrector process, (4.35) is solved using N-R method with initial conditions obtained from (4.34). Local parameterization is used in which additional equation specifying state variable value is augmented to original set of equations [27].

$$\begin{bmatrix} F(\delta, V, \lambda) \\ \lambda - \eta \end{bmatrix} = 0 \tag{4.35}$$

Where, η is the value of state variable λ. In the CPF method, there is an extra state variable λ than that in multiple load flow method. Therefore, the number of equations to be solved using this method is n_s+1 while that using multiple load flow method is n_s. Following three cases are observed using CPF method.

4.8.1 PV Curve with Continuous Power Flow Method

The CPF as described in section 4.8 is implemented for IEEE 9 bus system using Matpower. PV curves for load buses are shown in Fig. 4.6. In CPF, singularity problem in multiple power flow method is eliminated and PV curve can be traced beyond the maximum loadability point. The drawback of CPF method is that, while solving the load flow with CPF, step length should be assigned. A suitable step length is to be chosen such that it can give the solution at all loading condition up to the critical point. If the step length is large, the solution might not converge and if the step length is too small it takes more iterations and more time to generate the output [42]. PV curve in Fig.4.7 is obtained with step length of 0.2.
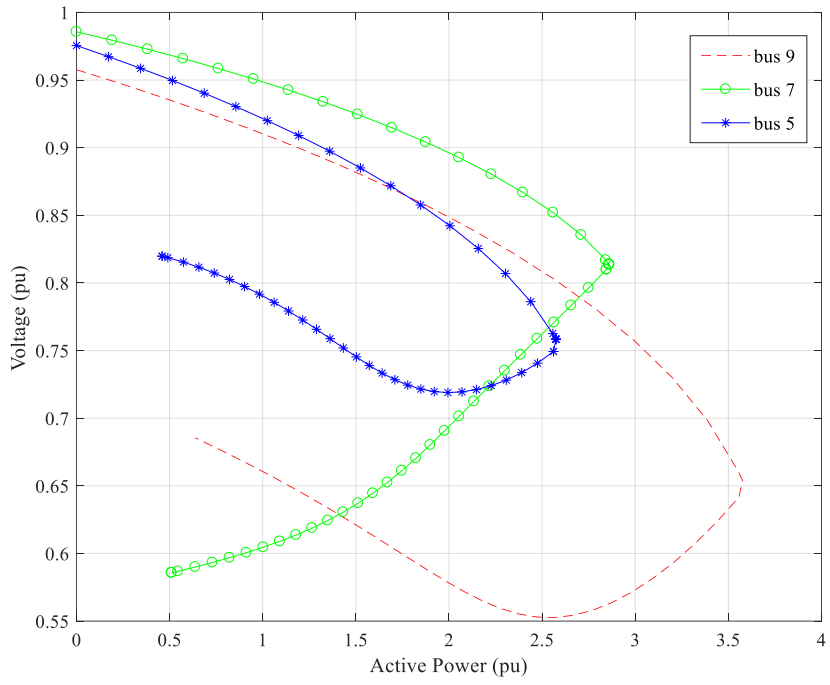
Fig. 4.6. Full PV curve using continuation method
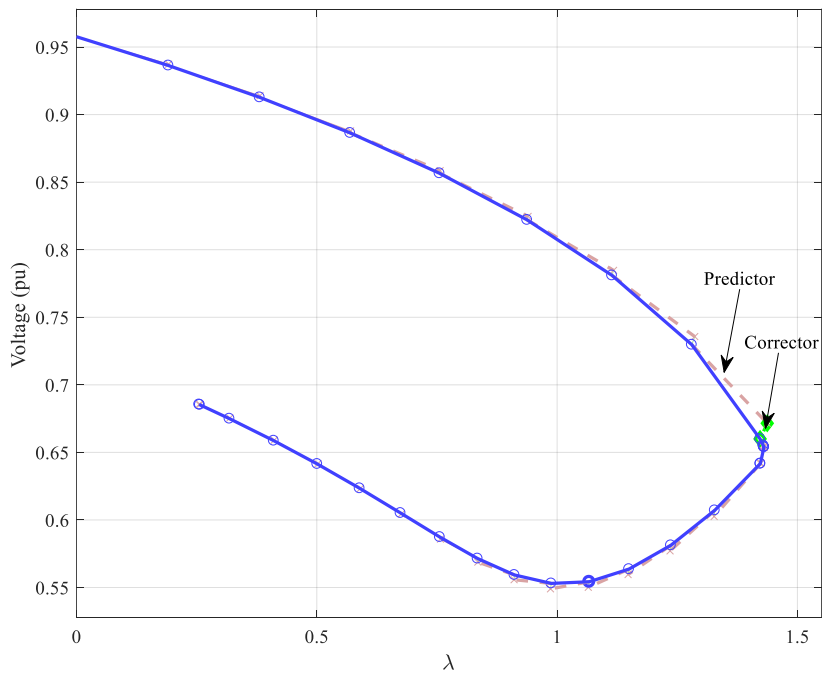
Fig. 4.7. Full V vs λ curve with step length 0.2
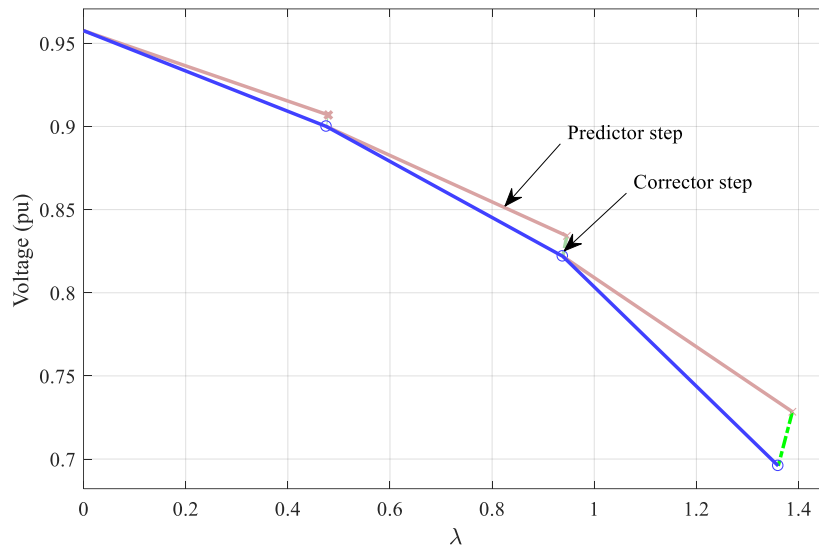
Fig. 4.8. V vs λ curve with step length 0.5

When the step length is changed to 0.5, the same problem fails to produce output at the critical

point as shown in Fig. 4.8. As a solution to this problem, adaptive step length is implemented in

Matpower. In this method of step length control, the step size is not fixed but it varies from given

minimum and maximum value. The exact step length in each iteration is calculated based on error

estimation between predicted and corrected solution.

4.8.2   Maximum Loadability using N-R Method and Continuous method
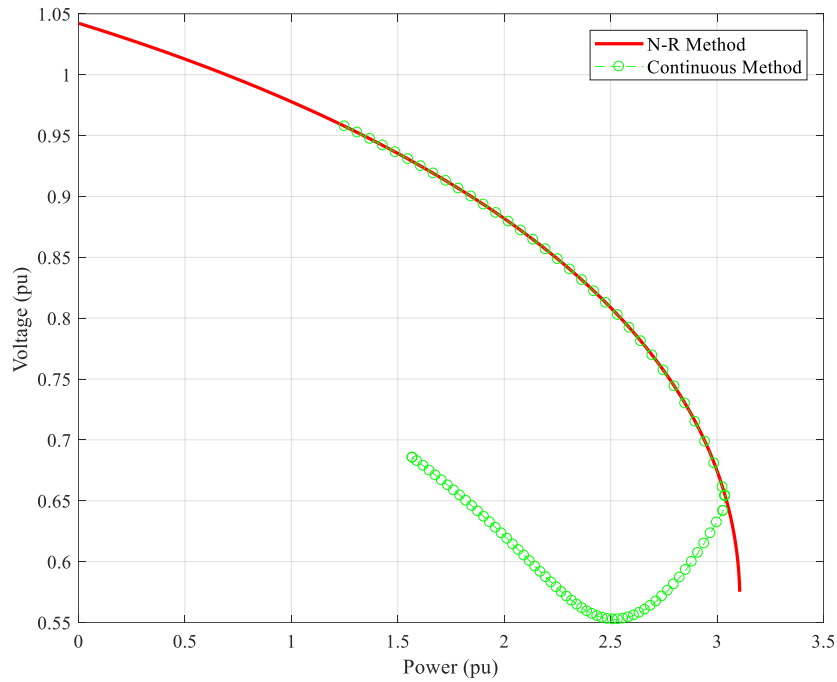
Fig. 4.9. Maximum loadability due to multiple load flow and CPF method

In Fig. 4.9, it is observed that the maximum loadability limit and minimum stable voltages are 3.106 p.u and 0.5752 p.u respectively. For CPF, the maximum loadability limit and minimum stable voltage while it is 3.038 p.u and 0.6542 p.u. This difference appears because of the numerical problem using multiple power flow method. When power flow reaches near the maximum loadability, the determinant of Jacobian matrix approaches to zero. The power flow solution obtained in such situation will not represent the true solution. However, this problem does not arise in CPF method.

4.8.3   Maximum Loadability for Constant Impedance and Constant Power Load

The maximum power capability of the power system can also be obtained using maximum power transfer theorem. Let us consider X be the reactance of transmission line in Fig. 4.1 and R_L be the connected load. Let us assume the resistance of transmission line is negligible and the power

factor of the load is one. According to maximum power transfer theorem, the source can deliver maximum power to the load when the value of the value of load resistance is equal to transmission line reactance. Maximum value of active power delivered is given by

$$P_{max} = \frac{E^2}{2R_L}$$

Or,

$$P_{max} = \frac{E^2}{2X} \qquad (4.36)$$
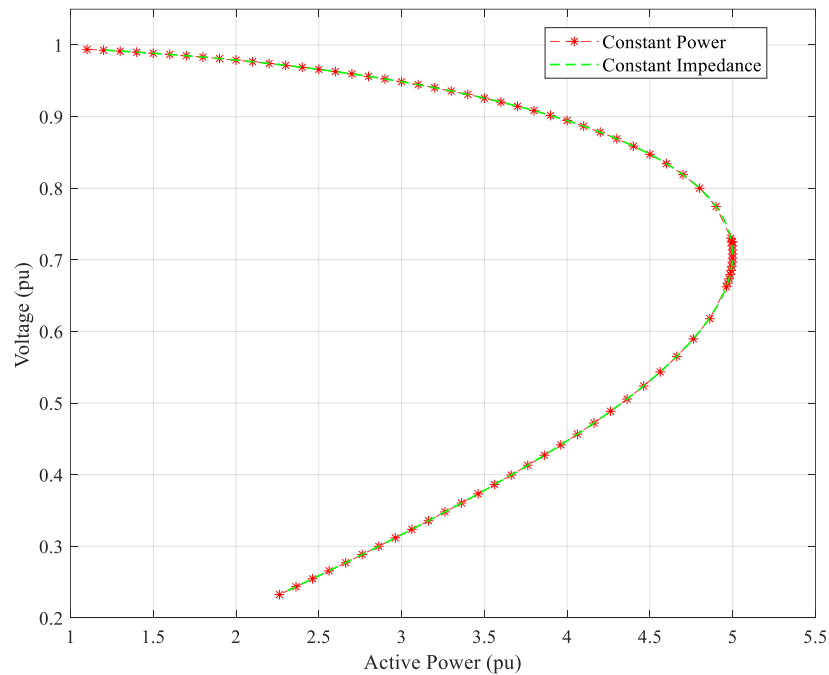
Fig. 4.10. Maximum Loadability for constant impedance and constant power load

Thus in uncontrolled case power system, the maximum power transfer capability is independent of characteristics of a load connected to it. This can be verified through PV curve obtained using CPF method for two bus system. As shown in Fig. 4.10. Two PV curves are obtained using two different types of load models namely constant power and constant impedance load. However, the maximum laudability can be increased (by changing the load characteristics seen at input terminal) for emergency situation implementing power electronics based loads (such as power

buffer) at the load side [44]. Next, the maximum value of power transferred also depends on the effective Thevenin's impedance seen at the load bus [1]. For larger Thevenin's impedance, PV curve shows lower maximum power transfer capability.

4.9   Concept Explanation for QV Curves

Another method of static voltage stability analysis is the V-Q sensitivity analysis [28]. In power system, the real power of bus is strongly linked with voltage angle and the reactive power is strongly coupled with voltage magnitude [26]. Linearized power flow equations (4.18) can be further simplified for V-Q sensitivity analysis. Assuming ΔP is zero, (4.18) can be modified as

$$\Delta Q = J_R \Delta V \tag{4.37}$$

$$\Delta V = J_R^{-1} \Delta Q \tag{4.38}$$

Where, J_R is reduced Jacobian matrix.

$$J_R = \left[J_{QV} - J_{Q\theta} J_{P\theta}^{-1} J_{PV} \right]$$

Positive V-Q sensitivity represents stable operation while negative V-Q represents unstable operation. V-Q sensitivity increases and becomes infinite at stability limit. This V-Q sensitivity can be analyzed and explained using Q-V curve for two bus system shown in Fig. 4.1. Q-V curve can be obtained with a similar procedure to PV curve. In PV curve, both P and Q were increased in a fixed ratio such that power factor remains constant. In Q-V curve, the value of P is kept constant and value of Q is varied in (4.24) and (4.25). The corresponding value of V and Q are plotted to obtain QV curve as shown in Fig. 4.11. This curve gives important information regarding reactive power injection required to maintain desired bus voltage. As shown in Fig. 4.11, if real power demand of the bus is 4 p.u it is required to supply a reactive power of 0.84 p.u to maintain bus voltage at 1.001 p.u. However, the system can supply 4 p.u active power and 0.5 p.u reactive power, if the voltage at load bus is kept at 0.8 p.u. Also, reactive power injection requirement decreases with a decrease in active power of the load.
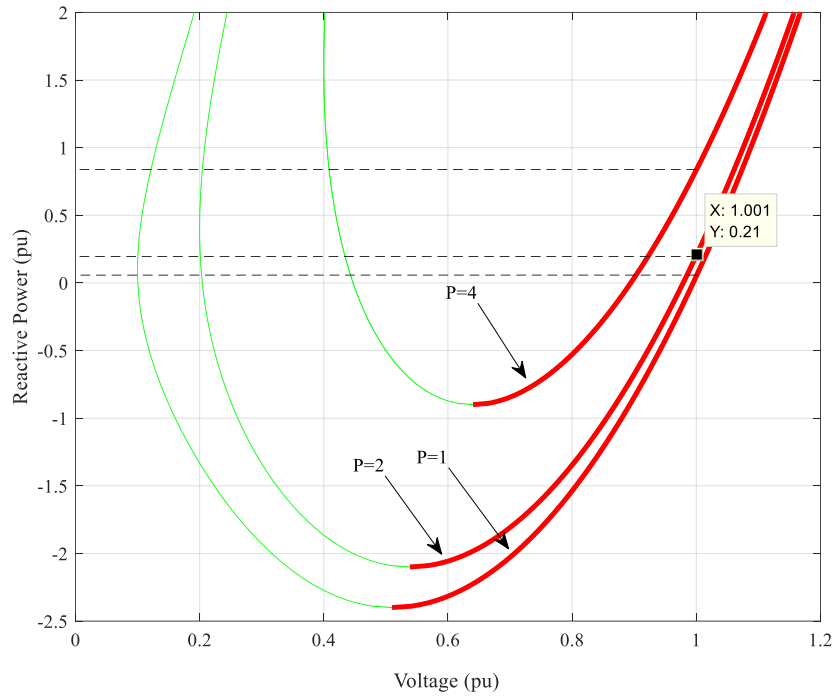
Fig. 4.11 Q-V curve for sensitivity analysis

This Q-V curve is used to determine the voltage stability through V-Q sensitivity analysis [4]. V-Q sensitivity is the ratio of change in bus voltage to change in reactive power of the bus and can be obtained from the derivative of Q-V curve. The system is stable if dQ/dV is positive while the system is unstable if dQ/dV is negative. Voltage stability limit is represented by the bottom of Q-V curves, where dQ/dV is zero. In the Fig. 4.11, the portion of the curve with bold solid line has positive V-Q sensitivity. This represents stable operating area of the system. The voltage of the system operating in this area can be increased by increasing reactive power injection at the bus. If the system is at unstable operating region, voltage of the system further decreases with increase in reactive power injection. Unstable operating region is shown by thin solid line in Fig. 4.11. The V-Q sensitivity at this region of operation is negative. The system at this point of operation can lead to voltage collapse if immediate corrective action is not taken by system operator. As a corrective action, the system operator can do load shedding on the bus as soon as it enters into unstable region of operation. From Fig. 4.11 it can be observed that for P equals to 4 p.u, minimum stable operating

43

voltage is 0.64 p.u, while that for P equals to 2 p.u is 0.53 p.u. As load is decreased to 2 p.u, the system becomes stable avoiding voltage collapse.

4.9.1   Determination of Most Sensitive Bus with QV Curves
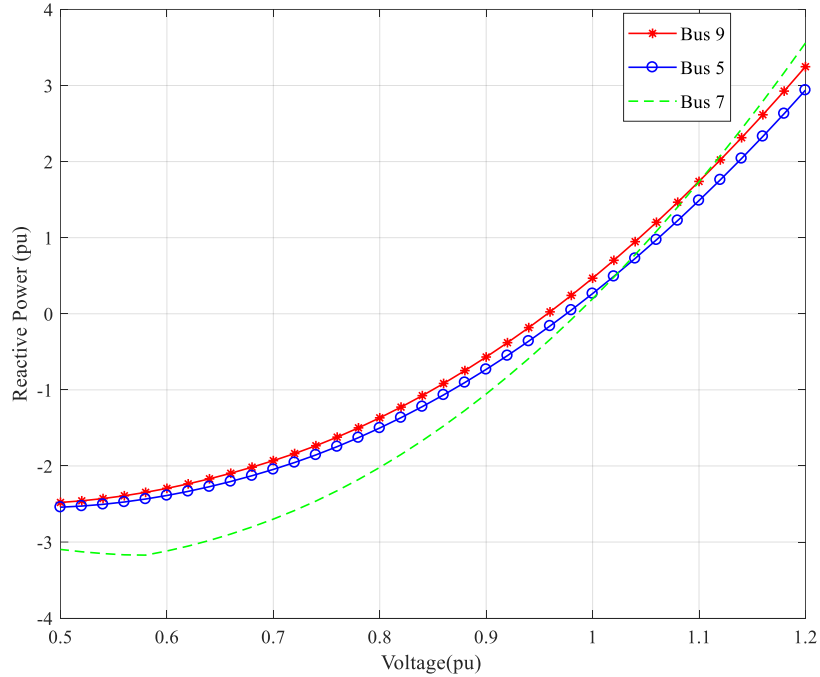
Fig. 4.12 Q-V curve for load buses in IEEE 9 bus system

Q-V curves for the load buses of IEEE 9 bus system are obtained in Fig. 4.12. It can be observed that bus 9 can supply 0.379 p.u of reactive power while it maintains minimum emergency bus voltage of 0.92 p.u. Bus 5 and bus 7 can supply 0.549 p.u and 0.827 p.u of reactive power to the load maintaining 0.92 p.u voltage at the corresponding buses. As it is known that at the stable operating region of Q-V curve, the bus voltage decreases with increase in reactive power of the load. Bus 9 can support minimum reactive power among the load buses at minimum emergency voltage condition. The connection of additional reactive power load at this bus significantly reduces the voltage that can result in voltage collapse. So, bus 9 is the most sensitive bus regarding the voltage collapse in IEEE 9 bus system.

CHAPTER V

DYNAMIC VOLTAGE STABILITY ANALYSIS

In static analysis, all the dynamics of connected devices are ignored and the system is assumed to be in perfect equilibrium. In this state, power generation exactly matches the demand and the bus voltage is maintained at a steady value. This assumption for static analysis holds true at the steady-state operation of power system. However, this assumption is not valid during the disturbances in power system. Various disturbances and single or multiple contingencies can trigger voltage instability phenomenon. So, to understand the mechanism of voltage instability in detail, it is essential to analyze the dynamic phenomenon of the power system.

In dynamic analysis, generators, excitation systems, turbine-governor systems, loads and other connected devices are modeled with differential equations while the transmission and distribution networks are modeled with algebraic equations. These sets of differential and algebraic equations make a complete mathematical model for dynamic analysis, which is then solved using one of the numerical solution techniques such as trapezoidal method, modified Euler's method etc. Dynamic analysis is required for transient and long-term stability analysis when there are large perturbations in power systems.

The mathematical modeling of the components determine the accuracy of the simulated

output. The modeling of the devices should be such that it closely represents the real systems. However, large systems require thousands of differential equations to be solved simultaneously which takes much time with existing computational capabilities of computers. So, the modeling of each component should be done such that the dynamic equations developed will be simple and accurate.

5.1 Mathematical Formulation for Dynamic Analysis

The network equations for dynamic analysis can be written nodal voltage form as

$$YV = I \tag{5.1}$$

Where,

$$
I = \begin{bmatrix} \begin{bmatrix} I_{x1} \\ I_{y1} \end{bmatrix} \\ \vdots \\ \begin{bmatrix} I_{x1} \\ I_{y1} \end{bmatrix} \\ \vdots \\ \begin{bmatrix} I_{x1} \\ I_{y1} \end{bmatrix} \end{bmatrix} \quad , V = \begin{bmatrix} \begin{bmatrix} V_{x1} \\ V_{y1} \end{bmatrix} \\ \vdots \\ \begin{bmatrix} V_{x1} \\ V_{y1} \end{bmatrix} \\ \vdots \\ \begin{bmatrix} V_{x1} \\ V_{y1} \end{bmatrix} \end{bmatrix}
$$

$$
Y = \begin{bmatrix} \begin{bmatrix} G_{11} & -B_{11} \\ B_{11} & G_{11} \end{bmatrix} & \cdots & \begin{bmatrix} G_{1i} & -B_{1i} \\ B_{11} & G_{11} \end{bmatrix} & \cdots & \begin{bmatrix} G_{1n} & -B_{1n} \\ B_{1n} & G_{1n} \end{bmatrix} \\ \vdots & & \vdots & & \vdots \\ \begin{bmatrix} G_{i1} & -B_{i1} \\ B_{i1} & G_{i1} \end{bmatrix} & \cdots & \begin{bmatrix} G_{ii} & -B_{ii} \\ B_{ii} & G_{ii} \end{bmatrix} & \cdots & \begin{bmatrix} G_{in} & -B_{in} \\ B_{in} & G_{in} \end{bmatrix} \\ \vdots & & \vdots & & \vdots \\ \begin{bmatrix} G_{n1} & -B_{n1} \\ B_{n1} & G_{n1} \end{bmatrix} & \cdots & \begin{bmatrix} G_{ni} & -B_{ni} \\ B_{ni} & G_{ni} \end{bmatrix} & \cdots & \begin{bmatrix} G_{nn} & -B_{nn} \\ B_{nn} & G_{nn} \end{bmatrix} \end{bmatrix}
$$

Where, I is the current injection vector, Y is admittance matrix and V is nodal voltage vector. Equation (5.1) is same as that used for the formulation of steady state equations in (4.1), except for dynamic simulation voltage vector, current vector and admittance matrix are represented in the Cartesian-coordinate form with the real and imaginary axis. This completes the network equation formulation for dynamic analysis.

Dynamic devices such as generators, loads and compensating devices are connected at various nodes of a network are linked together by a transmission network. At any time of operation, current injection into the network follows Kirchhoff's current law at each node. To solve the network variables, the equations form the dynamic devices and the network equations need to be solved simultaneously. So, the equations of synchronous generators, loads and other connected dynamic devices should be formulated such that it can be solved simultaneously with network equations.

5.1.1 Equation Formulation of Synchronous Generator

The terminal voltage of synchronous generator in synchronous rotating frame is given by (5.2), in which a generator is represented as a sub-transient voltage source behind sub-transient reactance.

$$\begin{bmatrix} V_d \\ V_q \end{bmatrix} = \begin{bmatrix} E_d'' \\ E_q'' \end{bmatrix} - \begin{bmatrix} R & X_q'' \\ X_d'' & R \end{bmatrix} \begin{bmatrix} I_d \\ I_q \end{bmatrix}$$

(5.2)

Coordinate transformation from synchronous rotating frame in d, q domain to x, y domain is given by

$$\begin{bmatrix} A_d \\ A_q \end{bmatrix} = \begin{bmatrix} \sin \delta & -\cos \delta \\ \cos \delta & \sin \delta \end{bmatrix} \begin{bmatrix} A_x \\ A_y \end{bmatrix}$$

(5.3)

Using (5.3), we change the equation (5.2) form d, q domain to x, y coordinate as (5.4) [34]

$$\begin{bmatrix} \sin \delta & -\cos \delta \\ \cos \delta & \sin \delta \end{bmatrix} \begin{bmatrix} V_x \\ V_y \end{bmatrix} = \begin{bmatrix} E_d'' \\ E_q'' \end{bmatrix} - \begin{bmatrix} R & X_q'' \\ X_d'' & R \end{bmatrix} \begin{bmatrix} \sin \delta & -\cos \delta \\ \cos \delta & \sin \delta \end{bmatrix} \begin{bmatrix} I_x \\ I_y \end{bmatrix}$$

(5.4)

After simplification, the injected current by the generator is obtained as

$$\begin{bmatrix} I_x \\ I_y \end{bmatrix} = \begin{bmatrix} g_x & b_x \\ b_y & g_y \end{bmatrix} \begin{bmatrix} E_d'' \\ E_q'' \end{bmatrix} - \begin{bmatrix} G_x & B_x \\ B_y & G_y \end{bmatrix} \begin{bmatrix} V_x \\ V_y \end{bmatrix}$$

(5.5)

Where,

$$g_x = \frac{R\sin\delta - X_d''\cos\delta}{R^2 + X_d''X_q''} \quad , \qquad b_x = \frac{R\cos\delta + X_q''\sin\delta}{R^2 + X_d''X_q''}$$

$$b_y = \frac{-R\cos\delta - X_d''\sin\delta}{R^2 + X_d''X_q''} \quad , \qquad g_y = \frac{R_a\cos\delta + X_q''\sin\delta}{R^2 + X_d''X_q''}$$

$$G_x = \frac{R - (X_d'' - X_q'')\sin\delta\cos\delta}{R^2 + X_d''X_q''} \quad , \qquad B_x = \frac{X_d''\cos^2\delta + X_q''\sin^2\delta}{R^2 + X_d''X_q''}$$

$$B_y = \frac{-X_d''\cos^2\delta - X_q''\sin^2\delta}{R^2 + X_d''X_q''} \quad , \qquad G_y = \frac{R - (X_d'' - X_q'')\sin\delta\cos\delta}{R^2 + X_d''X_q''}$$

Equation (5.5) can be substituted into (5.1) and after simplifications we get the equivalent injected current by the generator as

$$\begin{bmatrix} I_x' \\ I_y' \end{bmatrix} = \begin{bmatrix} g_x & b_x \\ b_y & g_y \end{bmatrix} \begin{bmatrix} E_d'' \\ E_q'' \end{bmatrix} \tag{5.6}$$

The following block of admittance matrix should be added to the network admittance matrix.

$$\begin{bmatrix} G_x & B_x \\ B_y & G_y \end{bmatrix}$$

5.1.2 Equation Formulation of Loads

Mathematical formulation of the equation for dynamic studies also needs to include the load models into the equation. Constant impedance type of loads is incorporated into network admittance matrix. Motor loads are also incorporated into network admittance matrix. However, admittance of motor loads varies with the change in a slip of a motor. Then, for motor loads network admittance matrix must be changed every time slip of motor changes.

Loads can be represented with static loads such as ZIP loads (3.9) and (3.10) or exponential loads (3.11) and (3.12). For any loads, the relation between current injection, power injection and node voltage is given by (5.7).

$$-P_i - jQ_i = V_i I_i^* \tag{5.7}$$

$$-P_i - jQ_i = (V_{xi} + jV_{yi})(I_{xi} - jI_{yi}) \tag{5.8}$$

Equating real and imaginary parts on each side we get,

$$\begin{bmatrix} -P_i \\ -Q_i \end{bmatrix} = \begin{bmatrix} V_{xi} & V_{yi} \\ -V_{yi} & V_{xi} \end{bmatrix} \begin{bmatrix} I_{xi} \\ I_{yi} \end{bmatrix} \tag{5.9}$$

The current injected due to load is given by (5.10)

$$\begin{bmatrix} I_{xi} \\ I_{yi} \end{bmatrix} = \frac{1}{V_{xi}^2 + V_{yi}^2} \begin{bmatrix} V_{xi} & -V_{yi} \\ V_{yi} & V_{xi} \end{bmatrix} \begin{bmatrix} -P_i \\ -Q_i \end{bmatrix} \tag{5.10}$$

5.2 Simulation Tools for Dynamic Voltage Stability Analysis

The simulation tool used for dynamic voltage stability analysis is Power System Simulator for Engineers (PSS/E). This is one of the most popular software used in utility industries mainly for transmission planning studies. This supports the static analysis such as power flow analysis, contingency analysis, etc. and dynamic analysis such as faults analysis, stability analysis, etc. PSS/E contains extensive libraries for generators and its control systems, protection relays, FACTs devices and static and dynamic load models [35].

PSS/E has capability to work in graphical user interface (GUI) mode as well as automation mode. Required data input for static analysis can be done through GUI window. However, the efficient method to input data to PSS/E is through data input files. So, all the required input data for this thesis work is given through input files in PSS/E. The input file must include information

about generation units, system network, loads and other components like transformers and reactive power compensating devices connected to the power system.

Dynamic simulation additionally requires dynamic file which contains the dynamic data of the components connected to the system. Then power flow solution is obtained before starting the dynamic simulation. Series of dynamic events are simulated, which produces output in channel output file. This file in binary format is used by PSS/E to produce a graphical output of the desired variables and states of power systems.

This complete process of dynamic simulation can be done using automation file. An automation file is a complete set of instructions using commands described in Application Program Interface (API) [45]. Automation file can be developed using IPLAN program or python program. This thesis work uses python program for automation of dynamic simulation.

5.3   Numerical Techniques for Dynamic Voltage Stability Analysis

Dynamic simulation is essential for power system planning and understanding the stability phenomenon in power system. Mathematical formulation of the network is presented in the previous section and the differential equations of generators and other connected devices are presented in chapter 3. This differential equation of each component and the algebraic equation of the network together called Differential Algebraic Equations (DAE) make a complete mathematical model of a power system. The set of DAE can be solved numerically to simulate the behavior of a power system. The set of dynamic equations from generating units and dynamic loads be represented by (5.11)

$$\dot{x} = f(x, y) \tag{5.11}$$

And the set of network equations be represented by (5.12)

$$0 = g(x, y) \tag{5.12}$$

The solution of these set of DAE determines the state of the system at any instant of time. Due to the disturbances in the power system, network configurations and the boundary conditions of the network change. This is modeled by changing the coefficient of the right-hand side of equations (5.7) and (5.8). The simulation should be able to calculate the solution at the different sequence of network disturbances.

Power system stores energy in the form of electromagnetic and electrostatic energy system, rotational inertia system and thermodynamic system [46]. Storage of electromagnetic and electrostatic energy is due to inductance and capacitance of the network and connected devices, which is discharged at an interval of 10^{-6} s to 10^{-3} s. This type of study is considered for switching and lighting overvoltage, which requires transient simulation of the system. Storage of rotational energy is due to the presence of rotating machines in the network such as generators and motor driven loads. This form of energy is discharged in the range of 0.1s to 10s. This type of energy storage system plays a significant role in the dynamic stability of power system. Also, the thermodynamic system of power plant involving the thermodynamic process of power plant operates at the range of 10 s to 10^{3} s.

Due to this large variation of time-frame of the power system, it is considered as a stiff system. The stiff system has large variations in time constants of the system components. This results in large variations in eigenvalues of the system. So the numerical technique used for the solution of power system should handle a stiff system.

The efficiency of simulation is determined by the time required by the simulation, which in fact depends on the numerical algorithm and the time step of the calculation. In addition, the integration method chosen should be efficient, convergent, stable, accurate, and capture desired dynamics of the power system. It is expected that the numerical solution gets closer to the analytical solution with the decrease in step size. This feature of the numerical solution is called convergent.

The numerical method gives convergent solution if it is consistent and stable. PSS/E uses modified Euler method for numerical integration. In the following section, consistency, stability, and convergence of modified Euler method are explored [47].

$$y' = f(x, y), \qquad y(x_0) = y_0 \tag{5.13}$$

In an initial value problem (5.13), let $y(x_n)$ be the analytical solution and Y_n be the numerical solution. Then,

$$\lim_{h \to 0} \max_n | y_n - Y_n| = 0 \tag{5.14}$$

Using simple Euler method in (5.13), we get (5.15)

$$\frac{Y_{n+1} - Y_n}{h} - f(x_n, Y_n) = 0 \tag{5.15}$$

$$F[Y_n - h] = 0 \tag{5.16}$$

Substituting Y_n by exact solution $y(x_n)$ we get,

$$F[y(x_n) - h] = \mathrm{T}_n \tag{5.17}$$

Where, T_n is discretization error. The numerical method is called consistent if

$$\lim_{h \to 0} \max_n | \mathrm{T}_n| = 0 \tag{5.18}$$

The consistent method sometimes fails to converge due to round-off error. Let the numerical solution with round-off error be U_n and without round-off error be Y_n. Then,

$$F[U_n - h] = \xi_n \tag{5.19}$$

Where, ξ_n is a small value due to round-off error. This error is expected to remain small, throughout the solution. The numerical solution is stable if

$$||U_n - Y_n|| \leq C||\xi_n|| \tag{5.20}$$

Where, C is constant depends on the length of step interval. The method is stable if the error in numerical solution doesn't grow with the number of steps. However, sometimes the value of ξ_n increases with computations, such types of numerical solutions are called unstable solution. A numerical method can also be partially stable, if the numerical method is stable only for certain value of λh. Let us consider an initial value problem (5.21)

$$y' = \lambda y, \quad re\ \lambda < 0, \quad y(x_0) = y_0 \tag{5.21}$$

Using Euler method in (5.21), we get,

$$Y_{n+1} = Y_n + \lambda h Y_n \tag{5.22}$$

$$Y_n = Y_0(1 + \lambda h)^n \tag{5.23}$$

The system is stable only if

$$|1 + \lambda h| < 1 \tag{5.24}$$

$$-1 < 1 + \lambda h < 1 \tag{5.25}$$

$$h < \frac{2}{|\lambda|} \tag{5.26}$$

Using modified Euler method, we get [47]

$$Y_{n+1} = Y_n + \frac{h}{2}[Y_n + Y'_{n+1}] \tag{5.27}$$

Where,

$$Y'_{n+1} = Y_n + \lambda h Y_n \tag{5.28}$$

$$Y_{n+1} = (1 + h\lambda + \frac{1}{2}(h\lambda)^2)Y_n \qquad (5.29)$$

The Euler method in (5.22) is modified to obtain modified Euler method in (5.29).The modified Euler method is stable if

$$\left|1 + h\lambda + \frac{1}{2}(h\lambda)^2\right| < 1 \qquad (5.30)$$

Let, $\lambda = \lambda_R + j\lambda_I$,

Then, stability region for modified Euler method is given in Fig. 5.1
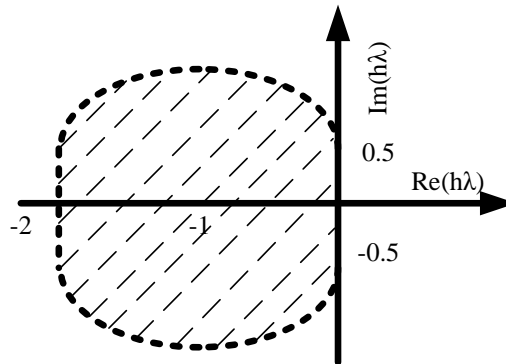
Fig. 5.1. Stable region of modified Euler integration method.

5.4   Power System Model for Dynamic Analysis

The test system shown in Fig. 5.2 will be used for dynamic voltage stability analysis. In this power system model, two generators G1 and G2 supply power to the network through step-up transformer T1 and T2 respectively. Power is supplied to two connected loads at bus 5, through two parallel transformers T3 and T4. The reactive power support at the load bus is provided by switched shunt capacitor Xc. The required data for dynamic analysis are given in Appendix.

Fig. 5.2. Five bus power system model.

5.5   Dynamic Voltage Stability with Load Modelling

Dynamic simulations are obtained using PSS\E. Generators are modeled as sixth order model [34] using GENROU model, exciters are modeled a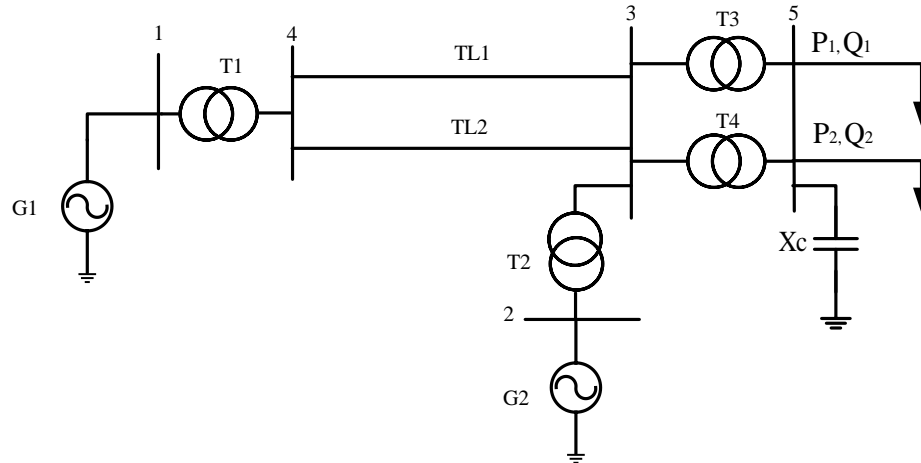s DC exciter as IEEET1 model, governors are modeled as steam turbine governor as TGOV3 and stabilizers are modeled as PSS2A model in PSS\E. The reactive power support at the load bus is supplied through switched shunt capacitor bank. Short-term voltage stability for different load models is presented and analyzed through fault-induced delayed voltage recovery (FIDVR). Due to FIDVR, system voltage gets depressed for a prolonged period of time after the fault is cleared [48]. It is mainly caused due to stalling of motor loads. Additionally, FIDVR is influenced by the point of a system fault, system voltage magnitude, fault clearance time, etc. FIDVR is a major reason for short-term voltage instability in power system.

1) FIDVR for constant impedance load and constant power loads.

In five bus system, a fault occurs at bus 5 and lasts for ten cycles before it is cleared. The static loads are modeled using IEEE load models in PSS\E. The frequency dependency of the load is ignored as it has minimum impact in voltage stability studies [49]. Fault-induced voltage recovery is obtained for ZIP load models.

The bus 5 voltage for constant impedance load and constant power load is shown in Fig. 5.3. It can be observed that the minimum voltage during the fault for constant power load is less than that of constant impedance load. Also, the voltage recovers faster for constant impedance load. This is because the power consumed by constant impedance load decreases at low voltage conditions while the constant power consumes constant power at low bus voltage conditions. Furthermore, it is expected that the real loads do not show their constant power characteristics at very low voltages. In this analysis, it is assumed that the constant power loads show its constant power characteristics when the bus voltage is more than 0.5 p.u. Below this voltage, the load acts as a constant current load.
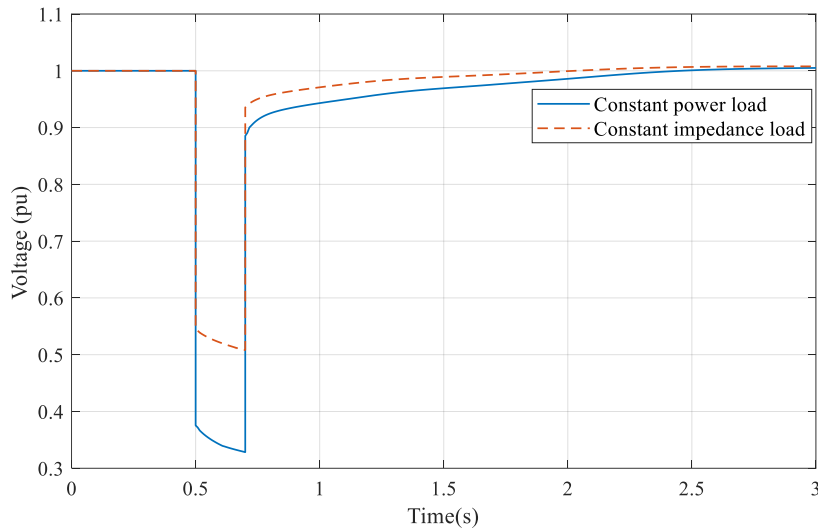
Fig. 5.3. Voltage at bus 5 due to static loads.

It can also be observed that in both cases in Fig. 5.3, bus voltage becomes higher than 0.9 p.u as soon as the fault is cleared, which is an acceptable voltage for emergency operating condition. FIDVR triggered by faults in transmission and sub-transmission lines were recorded using PMU in various substations of Southern California Edison. It was found that the voltage did not recover to 0.9 p.u for several seconds after faults were cleared [50]. Also, in some cases, voltage did not recover leading to voltage collapse. This delayed voltage recovery and the voltage collapse is

attributed to dynamic loads connected in the actual system.

2) *FIDVR for constant power loads and motor loads.*

In this case, FIDVR is compared between constant power load and motor loads. Motor load is modeled using complex load model in PSS\E. In this model, the percentage contribution of the motor load is 80 percent and remaining loads are constant impedance type of loads. It can be observed in Fig. 5.4, that the motor loads restores to 0.9 p.u after 0.83s from the instant fault is cleared. However, the constant power load recovers to 0.9 p.u voltage instantly after the fault is cleared. This is because the motor loads stall at low voltages. During the stalling of motors, the reactive power demand is high. When the fault is cleared, the motor takes a certain time to restore to normal operating conditions from the stalling condition. Also, it was observed that the critical clearing time for constant power load was 0.866 s while that of the motor load was 0.166 s. This shows that the delayed voltage recovery in the actual system is attributed to motor loads.
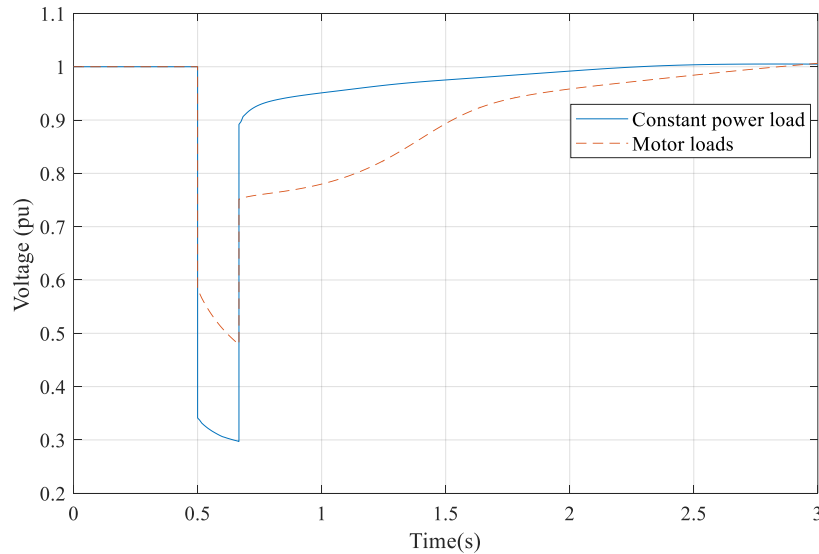

Fig. 5.4. Voltage at bus 5 due to motor loads and static loads.

3) *FIDVR for small motor loads and large motor loads.*

In actual power systems, various types of motor loads are connected. The characteristics of

different types of motor loads cannot be represented by a single model of motor load. In this case, separate models for small motors and large motors are modeled and their performances are evaluated. The critical clearing time for large motor loads was observed to be 0.1 s while that of the small motor load was 0.166 s. In Fig. 5.5, it can be observed that the small motor model rides through the fault and recovers to normal voltage after the clearance of fault. However, the voltage due to large motor loads progressively decreases after the clearance of fault which leads to voltage collapse.
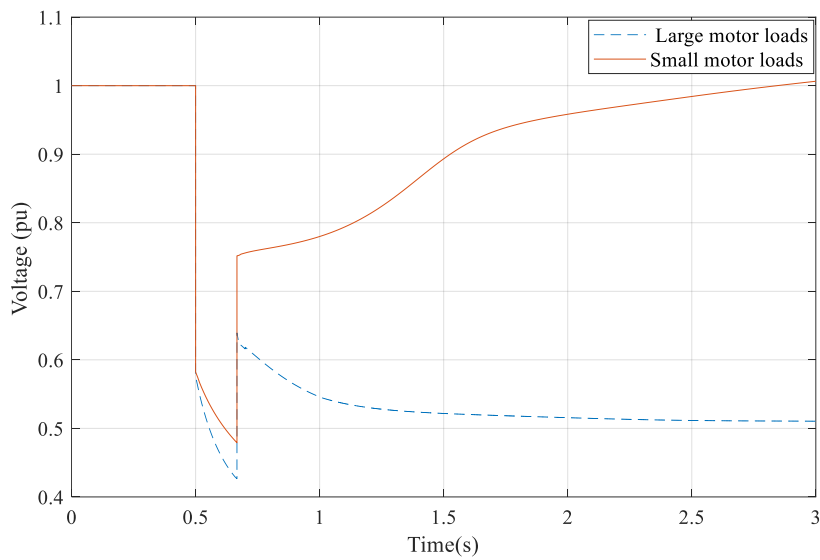
Fig. 5.5. Voltage at bus 5 due to small motor loads and large motor loads.

5.6   Voltage Restoration with Load Modelling

FIDVR for large motor loads and improved motor loads.

As a solution to voltage collapse due to large motor loads, the characteristics of other loads connected along with the motor loads are changed and the combination is called as improved motor loads. In the modeling of large motor loads, the other loads connected to the system are constant impedance loads. The voltage collapse occurs after the fault when the connected load is the combination of motor load and constant impedance load. However, when the load combination is changed and the large motor loads are connected in combination with the discharge lighting loads,

the critical clearing time increased from 0.1 s to 0.166 s. The system restores to normal voltage for the fault that existed for 10 cycles and the problem of voltage collapse is avoided for large motor loads.

Fig. 5.6. Voltage at bus 5 due to large motor loads and improved motor loads.

CHAPTER VI

CONCLUSIONS

In this thesis, static and dynamic analysis of voltage stability was performed. The static analysis carried out is based on load flow solutions with PV curves and QV curves. Maximum loadability of a nine bus power system was determined using multiple power flow method and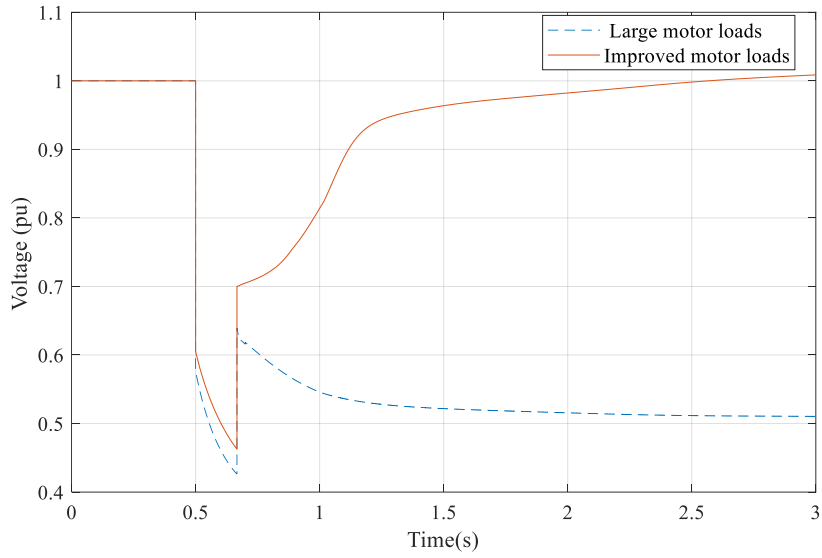 continuous power flow method. The minimum stable voltage and maximum loadability obtained using two techniques were different. This difference was attributed to the numerical problem using N-R method near the maximum loadability. The maximum loadability largely depends on the power factor of the load but it is independent of the types of static loads connected to it unless the power factor of the load changes. Also, based on the calculation of minimum reactive power that can be supplied by the corresponding bus at emergency minimum voltage conditions, the most sensitive load bus was determined using QV sensitivity analysis.

The short-term voltage stability due to fault was analyzed for a five bus power system model. Different types of load models were connected to a load bus and fault-induced delayed voltage recovery was analyzed. One main conclusion made here was that short-term voltage stability of the power system largely depends on the types of loads connected to the system. In static loads, constant power loads are more susceptible to voltage instability phenomenon than constant impedance type of loads. Furthermore, dynamic loads such as motor loads can further aggravate the voltage instability mechanism. This instability due to motor load is attributed to the

stalling of motors at low voltage conditions. However, when the combination of loads connected to the bus was changed, the voltage collapse due to the large motor was prevented. Thus, this can be one of the solutions to reduce voltage instability of the power system. As a future work, complex load model can be modified to include other major loads such as air conditioner loads, heating loads and the distributed generation units. Such modified load models can be used to assess the short term and long term voltage stability of power systems.

REFERENCES

[1]   W. W. Weaver and P. T. Krein, "Game-Theoretic Control of Small-Scale Power Systems," *IEEE Trans. Power Del.,* vol. 24, no. 3, pp. 1560-1567, 2009.

[2]   G. Andersson *et al.*, "Causes of the 2003 major grid blackouts in North America and Europe, and recommended means to improve system dynamic performance," *IEEE Trans. Power Syst.,* vol. 20, no. 4, pp. 1922-1928, 2005.

[3]   S. Chakrabarti, "Static load modelling and voltage stability indices," *Int. J. Elect. Power Energy Syst,* vol. 29, no. 3, pp. 200-5, 2009.

[4]   T. Van Cutsem, "Voltage instability: phenomena, countermeasures, and analysis methods," *Proc. IEEE,* vol. 88, no. 2, pp. 208-227, 2000.

[5]   S. L. Kabir, A. H. Chowdhury, M. Rahman, and J. Alam, "Inclusion of slack bus in Newton Raphson load flow study," in *Proc. Int. Conf. Elect. Comput. Eng.(ICECE)*, 2014, pp. 282-284.

[6]   V. Ajjarapu and C. Christy, "The continuation power flow: a tool for steady state voltage stability analysis," *IEEE Trans. Power Syst.,* vol. 7, no. 1, pp. 416-423, 1992.

[7]   T. Overbye, "Effects of load modelling on analysis of power system voltage stability," *Int. J. Elect. Power Energy Syst,* vol. 16, no. 5, pp. 329-338, 1994.

[8]   V. Ajjarapu and B. Lee, "Bifurcation theory and its application to nonlinear dynamical phenomena in an electrical power system," *IEEE Trans. Power Syst.,* vol. 7, no. 1, pp. 424-431, 1992.

[9]   W. D. Rosehart and C. A. Cañizares, "Bifurcation analysis of various power system models," *Int. J. Elect. Power Energy Syst,* vol. 21, no. 3, pp. 171-182, 1999.

[10]   H. A. Pulgar-Painemal and P. W. Sauer, "Bifurcations and loadability issues in power systems," in *Proc. IEEE Bucharest Power Tech*, 2009, pp. 1-6.

[11]   X. Li and C. Cañizares, "Chaotic behavior observations in a power system model," in *Proc. IEEE Bucharest Power Tech*, 2009, pp. 1-5.

[12]   K. Srivastava and S. Srivastava, "Elimination of dynamic bifurcation and chaos in power systems using facts devices," *IEEE Trans. Circuits Syst. I, Fundam. Theory,* vol. 45, no. 1, pp. 72-78, 1998.

[13]   W. Price *et al.*, "Load representation for dynamic performance analysis," *IEEE Trans. Power Syst.,* vol. 8, no. 2, pp. 472-482, 1993.

[14]   W. Price *et al.*, "Bibliography on load models for power flow and dynamic performance simulation," *IEEE Power Eng. Rev.,* vol. 15, no. 2, p. 70, 1995.

[15]   O. Abdalla, M. Bahgat, A. Serag, and M. El-Sharkawi, "Dynamic load modelling and aggregation in power system simulation studies," in *Proc. Middle-East Power syst. Conf.*, 2008, pp. 270-276.

[16]   D. J. Hill, "Nonlinear dynamic load models with recovery for voltage stability studies," *IEEE Trans. Power Syst.,* vol. 8, no. 1, pp. 166-176, 1993.

[17]   G. Morison, B. Gao, and P. Kundur, "Voltage stability analysis using static and dynamic approaches," *IEEE Trans. Power Syst.,* vol. 8, no. 3, pp. 1159-1171, 1993.

[18]   A. Arif, Z. Wang, J. Wang, B. Mather, H. Bashualdo, and D. Zhao, "Load Modeling – A Review," *IEEE Trans. Smart Grid,* To be published. 2017.

[19]   K. Rudion, H. Guo, H. Abildgaard, and Z. Styczynski, "Non-linear load modeling—Requirements and preparation for measurement," in *Proc. IEEE Power Energy Soc. Gen. Meeting*, 2009, pp. 1-7.

[20]   S. Zhu, Z. Dong, K. Wong, and Z. Wang, "Power system dynamic load identification and stability," in *Proc. Int. Conf. Power Syst. Tech. (POWERCON)*, 2000, vol. 1, pp. 13-18.

[21]   K. Morison, H. Hamadani, and L. Wang, "Practical issues in load modeling for voltage stability studies," in *Proc. IEEE Power Energy Soc. Gen. Meeting*, 2003, vol. 3, pp. 1392-1397.

[22]   B. Zhao, Y. Tang, W.-c. Zhang, and Q. Wang, "Modeling of common load components in power system based on dynamic simulation experiments," in *Proc. Int. Conf. Power Syst. Tech. (POWERCON)*, 2010, pp. 1-7.

[23]   K. Tomiyama *et al.*, "Modeling of load during and after system faults based on actual field data," in *Proc. IEEE Power Energy Soc. Gen. Meeting*, 2003, vol. 3, pp. 1385-1391.

[24]   W. Xu and Y. Mansour, "Voltage stability analysis using generic dynamic load models," *IEEE Trans. Power Syst.,* vol. 9, no. 1, pp. 479-493, 1994.

[25]   W. W. Weaver and P. T. Krein, "Mitigation of power system collapse through active dynamic buffers," in *Proc. IEEE Power Electron. Specialists Conf.*, 2004, vol. 2, pp. 1080-1084.

[26]   P. Kundur, N. J. Balu, and M. G. Lauby, *Power system stability and control*. McGraw-hill New York, 1994.

[27]   V. Ajjarapu, *Computational Techniques for Voltage Stability Assessment and Control*. Springer US, 2007.

[28]   C. W. Taylor, *Power system voltage stability*. McGraw-Hill, 1994.

[29]   M. Eremia and M. Shahidehpour, *Handbook of electrical power system dynamics: modeling, stability, and control*. John Wiley & Sons, 2013.

[30]   X. F. Wang, Y. Song, and M. Irving, *Modern Power Systems Analysis*. Springer US, 2010.

[31]   T. Van Cutsem and C. Vournas, *Voltage stability of electric power systems*. Springer Science & Business Media, 1998.

[32] N. C. Ekneligoda and W. W. Weaver, "A Game Theoretic Bus Selection Method for Loads in Multibus DC Power Systems," *IEEE Trans. Ind. Electron.,* vol. 61, no. 4, pp. 1669-1678, 2014.

[33] W. W. Weaver and P. T. Krein, "Distributed dynamic energy resource control," in *Proc. IEEE Elect. Ship Technol. Symp.*, 2009, pp. 182-188.

[34] M. Jan, W. Janusz, and R. James, "Power system dynamics: Stability and Control," *John Wily and Sons,* 2008.

[35] *Siemens Inc. PSS/E 34 Model Library*. 2015.

[36] D. Kosterev, "Composite load model development and implementation," presented at the NERC-DOE FIDVR Conf., 2015.

[37] *Siemens Inc. PSS/E 31.0 Program Operation Manual*. 2015.

[38] H. Saadat, *Power System Analysis*. McGraw-Hill, 1999.

[39] T. H. Chen, M. S. Chen, K. J. Hwang, P. Kotas, and E. A. Chebli, "Distribution system power flow analysis-a rigid approach," *IEEE Trans. Power Del.,* vol. 6, no. 3, pp. 1146-1152, 1991.

[40] W. Marszalek and Z. W. Trzaska, "Singularity-induced bifurcations in electrical power systems," *IEEE Trans. Power Syst.,* vol. 20, no. 1, pp. 312-320, 2005.

[41] R. D. Zimmerman, C. E. Murillo-Sanchez, and R. J. Thomas, "MATPOWER: Steady-State Operations, Planning, and Analysis Tools for Power Systems Research and Education," *IEEE Trans. Power Syst.,* vol. 26, no. 1, pp. 12-19, 2011.

[42] S. G. Ghiocel and J. H. Chow, "A Power Flow Method Using a New Bus Type for Computing Steady-State Voltage Stability Margins," *IEEE Trans. Power Syst.,* vol. 29, no. 2, pp. 958-965, 2014.

[43] R. Seydel, *Practical bifurcation and stability analysis*. Springer Science & Business Media, 2009.

[44] W. W. Weaver and P. T. Krein, "Optimal Geometric Control of Power Buffers," *IEEE Trans. Power Electron.,* vol. 24, no. 5, pp. 1248-1258, 2009.

[45] *Siemens Inc. PSS/E 34 Application Program Interface*. 2015.

[46] *Siemens Inc. PSS/E 34 Program Application Guide Volume 1*. 2015.

[47] R. Hamming, *Numerical methods for scientists and engineers*. Courier Corporation, 2012.

[48] K. Zhang, H. Zhu, and S. Guo, "Dependency analysis and improved parameter estimation for dynamic composite load modeling," *IEEE Trans. Power Syst.,* vol. 32, no. 4, pp. 3287-3297, 2017.

[49] W. E. C. Council, "Guide to WECC/NERC planning standards ID: voltage support and reactive power," 2006.

[50] R. J. Bravo, R. Yinger, and P. Arons, "Fault induced delayed voltage recovery (FIDVR) indicators," in *Proc. IEEE PES Transmission and Distribution Conf. Expo.*, 2014, pp. 1-5.

APPENDICES

Power flow data for IEEE 9 bus system

BUS DATA					
BUS	TYPE	$V(pu)$	$\delta(deg)$	P	Q
1	Slack	1.00	0.00	71.95	24.07
2	PV	1.00	9.669	163.00	14.46
3	PV	1.00	4.771	85.00	-3.65
4	PQ	0.987	-2.407	0.00	0.00
5	PQ	0.975	-4.017	-90.00	-30.00
6	PQ	1.003	1.926	0.00	0.00
7	PQ	0.986	0.622	-100.00	-35.00
8	PQ	0.996	3.799	0.00	0.00
9	PQ	0.958	-4.350	-125.00	-50.00

Branch data for IEEE 9 bus system

FROM BUS	TO BUS	$R(pu)$	$X(pu)$	$B(pu)$
1	4	0.000	0.0576	0.000
4	5	0.017	0.092	0.158
5	6	0.039	0.17	0.358
3	6	0.000	0.0586	0.000
6	7	0.0119	0.1008	0.209
7	8	0.0085	0.072	0.149
8	2	0.000	0.0625	0.000
8	9	0.032	0.161	0.306
9	4	0.01	0.085	0.176

Power flow data for Five bus system

BUS DATA					
BUS	TYPE	$V(pu)$	$\delta(deg)$	P	Q
1	Slack	1.025	0.00	164.66	7.61
2	PV	1.040	-6.576	71.64	43.97
3	PQ	1.014	-9.008	0.00	0.00
4	PQ	1.025.	-5.180	0.00	0.00
5	PQ	1.000	-12.900	-235.00	-141.50

Branch data for Five bus system

FROM BUS	TO BUS	$R(pu)$	$X(pu)$	$B(pu)$
1	4	0.000	0.0576	0.000
2	3	0.000	0.0625	0.000
3	4	0.01	0.085	0.176
3	4	0.01	0.085	0.176
3	5	0.000	0.0586	0.000
3	5	0.000	0.0586	0.000

Initially switched shunt at bus 5 is 100 MVAR

Generator data

$T'_{do}(s)$	$T''_{do}(s)$	$T'_{qo}(s)$	$T''_{qo}(s)$	H	D	X_d	X_q
6.00	0.05	0.535	0.05	9.33	0.67	1.72	1.66

X'_d	X'_q	$X''_d = X''_q$	$X1$	$S(1.0)$	$S(1.2)$
0.23	0.37	0.21	0.10	1.01	1.02

Excitation system data

T_R	K_A	T_A	V_{RMAX}	V_{RMIN}	K_E	T_E	K_F	T_F
0.0 -	20.0	0.2	3.0	-3.0	1.0	0.314	0.063	0.35

$E1$	$SE(E1)$	$SE(E2)$	$E2$	$SE(E1)$
0.0	2.8	0.3034	3.73	1.2884

Governor system data

K	T_1	T_2	T_3	U_0	U_C	P_{MAX}	P_{MIN}	T_4
20	0.9	0.2	0.5	0.1	-0.1	1	0	0.2

K_1	T_5	K_2	T_6	K_3	T_A	T_B	T_C	P_{RMAX}
0.5	0.2	0.3	0.2	0.2	0.1	0.3	1.5	1

Complex load model data

R	X	P_0	K_p
0.05	0.1	235	2

VITA

KISHOR GAIRE

Candidate for the Degree of

Master of Science

Thesis: IMPACT OF LOAD MODELING ON POWER SYSTEM VOLTAGE STABILITY

Major Field: Electrical Engineering

Biographical:

Education:

Completed the requirements for the Master of Science in Electrical Engineering at Oklahoma State University, Stillwater, Oklahoma in December, 2017.

Completed the requirements for the Bachelor of Science in Electrical Engineering at Tribhuvan University, Kathmandu, Nepal in 2011.

Experience:

Graduate Research Assistant with Dr. Nishantha Ekneligoda in the School of Electrical and Computer Engineering at Oklahoma State University.

Electrical Engineer at Nepal Electricity Authority, Rupandehi, Nepal

Assistant Lecturer at Advanced College of Engineering and Management, Kathmandu, Nepal

Professional Memberships: IEEE Student Member
                          Registered Engineer, Nepal Engineering Council